USGS
science for a changing world

Reconnaissance Sediment Budget for Selected Watersheds of West Maui, Hawai‘i

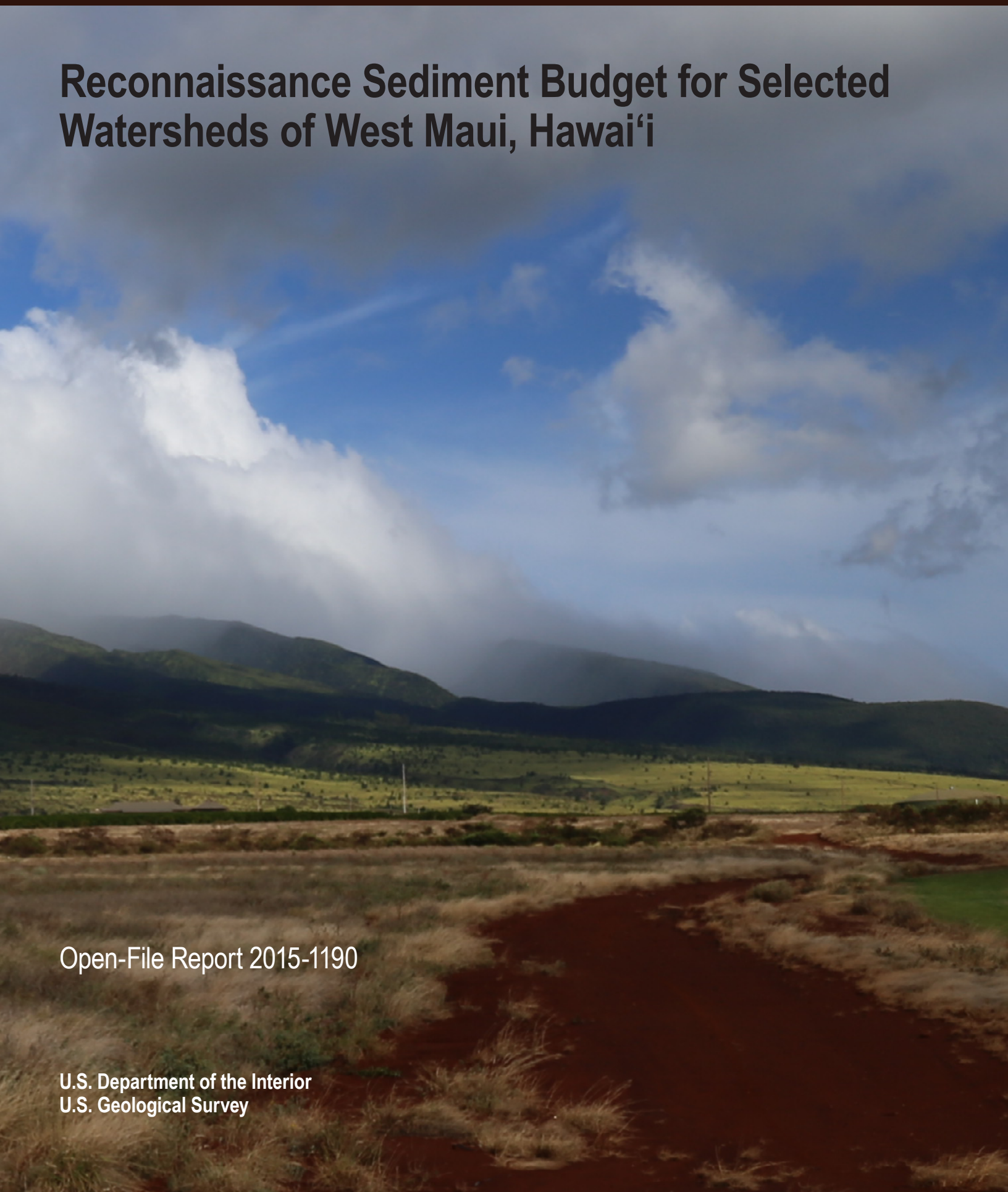

Open-File Report 2015-1190

U.S. Department of the Interior
U.S. Geological Survey

Cover. Photograph of low-intensity trade-wind rainfall over Honokōwai watershed, West Maui, Hawai‘i.

Reconnaissance Sediment Budget for Selected Watersheds of West Maui, Hawai‘i

By Jonathan D. Stock, Kim A. Falinski, and Tova Callender

Open-File Report 2015–1190

U.S. Department of the Interior
U.S. Geological Survey

U.S. Department of the Interior
SALLY JEWELL, Secretary

U.S. Geological Survey
Suzette M. Kimball, Director

U.S. Geological Survey, Reston, Virginia: 2016

For more information on the USGS—the Federal source for science about the Earth, its natural and living resources, natural hazards, and the environment—visit http://www.usgs.gov or call 1–888–ASK–USGS.

For an overview of USGS information products, including maps, imagery, and publications, visit http://www.usgs.gov/pubprod/.

Suggested citation:
Stock, J.D., Falinksi, K.A., Callender, T., 2016, Reconnaissance sediment budget for selected watersheds of West Maui, Hawai'i: U.S. Geological Survey Open-File Report 2015–1190, 42 p., http://www.dx.doi.org/10.3133/ofr20151190.

ISSN 2331-1258 (online)

Contents

Figures

Tables

Conversion Factors

[International System of Units to Inch/Pound]

Multiply	By	To obtain
	Length	
centimeter (cm)	0.3937	inch (in.)
millimeter (mm)	0.03937	inch (in.)
meter (m)	3.281	foot (ft)
kilometer (km)	0.6214	mile (mi)
meter (m)	1.094	yard (yd)
	Area	
square meter (m^2)	0.0002471	acre
square kilometer (km^2)	247.1	acre
square meter (m^2)	10.76	square foot (ft^2)
square kilometer (km^2)	0.3861	square mile (mi^2)
	Volume	
cubic meter (m^3)	264.2	gallon (gal)
cubic meter (m^3)	0.0002642	million gallons (Mgal)
cubic meter (m^3)	35.31	cubic foot (ft^3)
cubic meter (m^3)	1.308	cubic yard (yd^3)
cubic meter (m^3)	0.0008107	acre-foot (acre-ft)
	Rate	
millimeter per hour (mm/hr)	0.03937	inch per hour (in/h)
millimeter per year (mm/a)	0.03937	inch per year (in/yr)
	Mass	
kilogram (kg)	2.205	pound avoirdupois (lb)
metric ton per year	1.102	ton per year (ton/yr)
	Density	
kilogram per cubic meter (kg/m^3)	0.06242	pound per cubic foot (lb/ft^3)

Slope in radians (α rad) may be converted to degrees (α°) as $\alpha^\circ = \arctan(\alpha \text{ rad})$

Reconnaissance Sediment Budget for Selected Watersheds of West Maui, Hawai‘i

By Jonathan D. Stock,[1] Kim A. Falinski,[2] and Tova Callender[3]

Abstract

Episodic runoff brings suspended sediment to the nearshore waters of West Maui, Hawai‘i. Even small rainfalls create visible plumes over a few hours. We used mapping, field experiments, and analysis of recent (July 19–20, 2014) and historic rainfall to estimate sources of land-based pollution for two watersheds in West Maui: Honolua, and Honokōwai. Former agricultural fields and some unimproved roads are plausible sources for polluted runoff, but have saturated hydraulic conductivities greater than the 10–15 millimeters per hour (mm/hr) rainfalls of July 2014. These fields and roads showed minor evidence for storm runoff, and could not have contributed substantially to July 2014 plume generation. Since 1978, rain at intensities capable of causing runoff from former agricultural fields sustained for 1–2 hours is also rare; such intensities have 2–5 year recurrence rates in the north, and greater than 25 year recurrence rates to the south near Lahaina. Streambanks now eroding into historic terraces of sands, silts, and clays are a more plausible source. Although past large storms contributed to sediment loading, annual plume generation is now caused by smaller rainfalls eroding these near-stream legacy deposits. Treatments of former agricultural fields, roads, and reserve forests are consequently not likely to measurably affect sediment pollution from smaller, more frequent storms. Increased runoff from the development of West Maui has the potential to exacerbate sediment plumes from such storms unless there is an effective strategy to reduce bank erosion. Uncertainties in the extent and erosion rate of historic terraces, however, limit our ability to plan mitigation.

Introduction

Coral ecosystems of West Maui have ecological, cultural, and recreational significance. A lucrative tourist industry provides economic benefit to the community. This enterprise depends on a healthy coral ecosystem, which is increasingly under threats from global climate change, marine resource use, and local land-based pollution. Sediment, nutrients, and other pollutants are transported to coastal waters in runoff, groundwater seepage, and atmospheric fallout. These pollutants degrade coral ecosystems by blocking light used for photosynthesis, inhibiting coral larval recruitment, smothering and abrading coral, and triggering increases in macroalgae. Although terrestrial pollution is one of many factors threatening coral reef survival, it is the one that local communities can profoundly influence.

We use mapping, field experiments, and data analysis to create a reconnaissance sediment budget for two large watersheds in West Maui: Honolua and Honokōwai (fig. 1). A sediment budget (see Dietrich and Dunne, 1978) is a table of sediment loads, typically arranged by geomorphic process. It enables users to focus mitigation on sediment sources about which they expect to be most concerned. These sources may be small areas producing disproportionately large amounts of sediments (such as hotspots), or sources of sediment whose supply rates might change dramatically as climate or land use change (for example, bank erosion from urbanized runoff). A sediment budget gives us the ability to forecast likely changes to sediment loading because we can assess the impact of such changes for each separate geomorphic process. Sediment budgets require maps of the extent of particular geomorphic processes and estimates of the rate of sediment production from each process. The total area and the erosion rate of each process are multiplied together and summed over all processes to create an annual sediment load from a watershed. The process maps are made by correlating field observations with topography or imagery, so that base maps can be used to generalize local field observations across the landscape. Erosion rates are estimated from monitoring data (for example, erosion pins and suspended-sediment and stream-gaging efforts) or isotopic methods (for example, cosmogenic radionuclides or ^{137}Cs). West Maui lacks U.S. Geological Survey suspended-sediment gages or other published work that estimates lowering rates from field observations. Without data on erosion rates, one cannot construct an authoritative sediment budget. Instead, we use erosion rates from elsewhere in Hawai‘i to create a

[1]U.S. Geological Survey.
[2]University of Hawai‘i at Mānoa.
[3]West Maui Ridge to Reef Initiative.

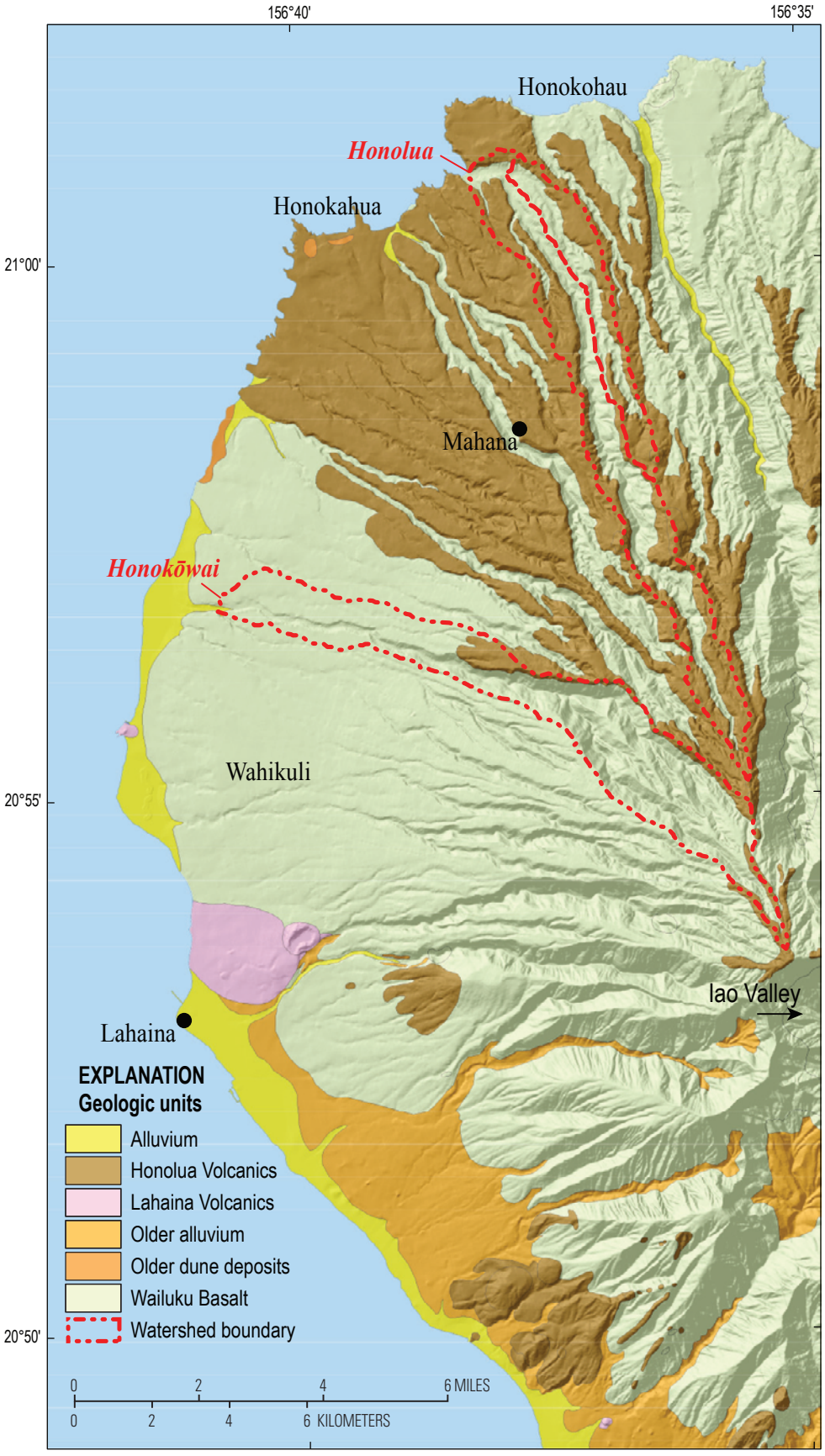

Base from U.S. Geological Survey 10-meter digital elevation model dataset
Universal Transverse Mercator, zone 4, North American Datum 1983

Figure 1. Map of geology of West Maui draped over shaded relief topography. Red lines show watershed boundaries of Honokōwai and Honolua and its major sub-watershed. Both watersheds have steep headwaters characterized by rockfall and landslide processes, with downvalley canyons cut into low-relief surfaces composed of volcanic and alluvial deposits. A cap of bright red-orange silts and fine sands over the volcanic units may be a source of sediment-rich plumes polluting the nearshore after rainfalls. Geology from Sherrod and others (2007).

reconnaissance sediment budget for West Maui. The term reconnaissance implies that further work with local erosion-rate estimates might modify the budget. In this spirit, our goal is to report the most necessary measurements in order to achieve a more authoritative estimate of the sources of fine-sediment pollution to the nearshore. Serendipitously, some of the hypotheses that we used to construct this reconnaissance budget can be tested against observations of active sediment transport during a recent runoff event.

We witnessed rainfalls on July 19–20, 2014 in West Maui. On the morning of July 20, we visited major stream outlets and coastal areas of West Maui, from Lahaina north to Honokōhau Stream (fig. 1), using public roadways. In the following days, we walked public lands or public access trails in selected West Maui watersheds. This allowed us to observe the effects of the July rainfalls on unimproved roads, trails, former agricultural fields, forests, and the valleys cutting through these areas. We were not able to access most West Maui watersheds owned by Maui Land and Pineapple Company (MLP) during our visit. We did accompany MLP field operations for one day after the storm, under the supervision of Pomaikaʻi Kaniaupio-Crozier, conservation manager for Puʻu Kukui Watershed Preserve, a division of MLP. As a consequence of this limited access, our reconnaissance mapping and sediment budget must be viewed with some reservations.

In the following sections, we describe the geology and geomorphology of West Maui. This geology sets the initial distribution of fine sediments across the landscape, and the geomorphology is a statement about how processes move these sediments. Neither is known well. We also recognize that differences in the geologic units affect landforms, weathering, and erosion rates, but these effects in Maui are yet to be fully explored.

We describe the field methods and data analysis we used to predict rainfalls that cause hillslope erosion, and the methods we used to map the geomorphic processes moving sediment. We present a speculative logic to estimate West Maui erosion rates using field data from elsewhere in Hawaiʻi. We describe field observations of the runoff from the July 19–20, 2014 storm event, and explore results of the rainfall analysis. Finally, we present the reconnaissance sediment budget for two watersheds and discuss pathways to a more authoritative budget. This work represents a preliminary effort to identify mitigation priorities, which we are following up with more detailed fieldwork for a U.S. Geological Survey (USGS) Scientific Investigations Map or Report.

Geology and Geomorphology

Stearns and Macdonald (1942) and more recently Sherrod and others (2007) reported on the geology of West Maui. Below we summarize these two sources. West Maui (fig. 1) was built as a basaltic shield by 1.3–2-Ma (million years ago) flows of the Wailuku Basalt. These lavas flowed from a central vent, now occupied by ʻĪao Valley, with rift zones marked by dikes that trend northward and south-southeastward. Flows dip steeply to the east and less steeply to the west. Stearns and Macdonald (1942) interpreted this asymmetry as boundary effect created by the presence of an island to the west (Molokaʻi) and the absence of an island to the east. Wailuku flows range from ~1 to 100 feet in thickness; unweathered flows are gray to gray blue. Pāhoehoe flows are interbedded with ʻaʻā flows and autobreccia layers. Some dikes are found at high angles to the original flow direction, appearing as lineaments that cut across valley slopes. Wailuku flows are capped by weathered saprolites and soil, with local alluvial deposits. Soils are dark red and reddish brown (Stearns and Macdonald, 1942).

The Honolua Volcanics are a postshield, 1.1–1.3-Ma series of trachyte and benmoreite volcanic flows overlying the Wailuku flows. The Honolua flows were erupted from magma with greater amounts of silica, potassium, and sodium than the Wailuku magmas (see figure 23 in Sherrod and others, 2007). Total reported thicknesses range from ~30 feet to more than 200 feet (Stearns and Macdonald, 1942); Patterson, 1971). The Honolua flows formed domes (sheet 7 in Sherrod and others, 2007), perhaps because magmas were more viscous than those of the Wailuku flows. Other surficial features, such as flow margins and pressure ridges, may also have higher relief than equivalent features in the less viscous Wailuku Basalt. Saprolites developed on the Honolua Volcanics are white and gray (Sherrod and others, 2007), and soils are light gray, brown gray, and white (Stearns and Macdonald, 1942). Long after this shield and postshield volcanism, four small eruptions occurred near Lahaina at ~0.3 Ma and ~0.6 Ma. Eruptions of the Lahaina Volcanics created four cones of low-silica content volcanics (basanites in this case), two of which released flows.

Valleys radiating from West Maui's center dissected rocks of the Wailuku Basalts, and overlying Honolua Volcanics. Low-relief remnants of lava-flow surfaces remain as wedge-shaped uplands, bounded by steep-sided valleys. Stearns and Macdonald (1942) called these remnants flow-slope plains; later workers (for example, Patterson, 1971) called them planeze. The northern watersheds are cut into both Honolua Volcanics and the underlying Wailuku Basalt. Starting near Honokōwai Stream and extending southward to Lahaina, watersheds are cut only in the older shield lavas of the Wailuku Basalt (fig. 1). Bright red-orange sands and silts can be found blanketing remnant flow surfaces of West Maui (fig. 2*A*). This material may have originated as air fall and other fragmental material, or from weathering of bedrock flows. It represents a prominent source of granular material now visibly appearing in coastal waters as suspended sediment. These well-sorted fine-sediments are locally overlain by a bouldery alluvium ~2–3 meters thick where exposed (fig. 2*B*).

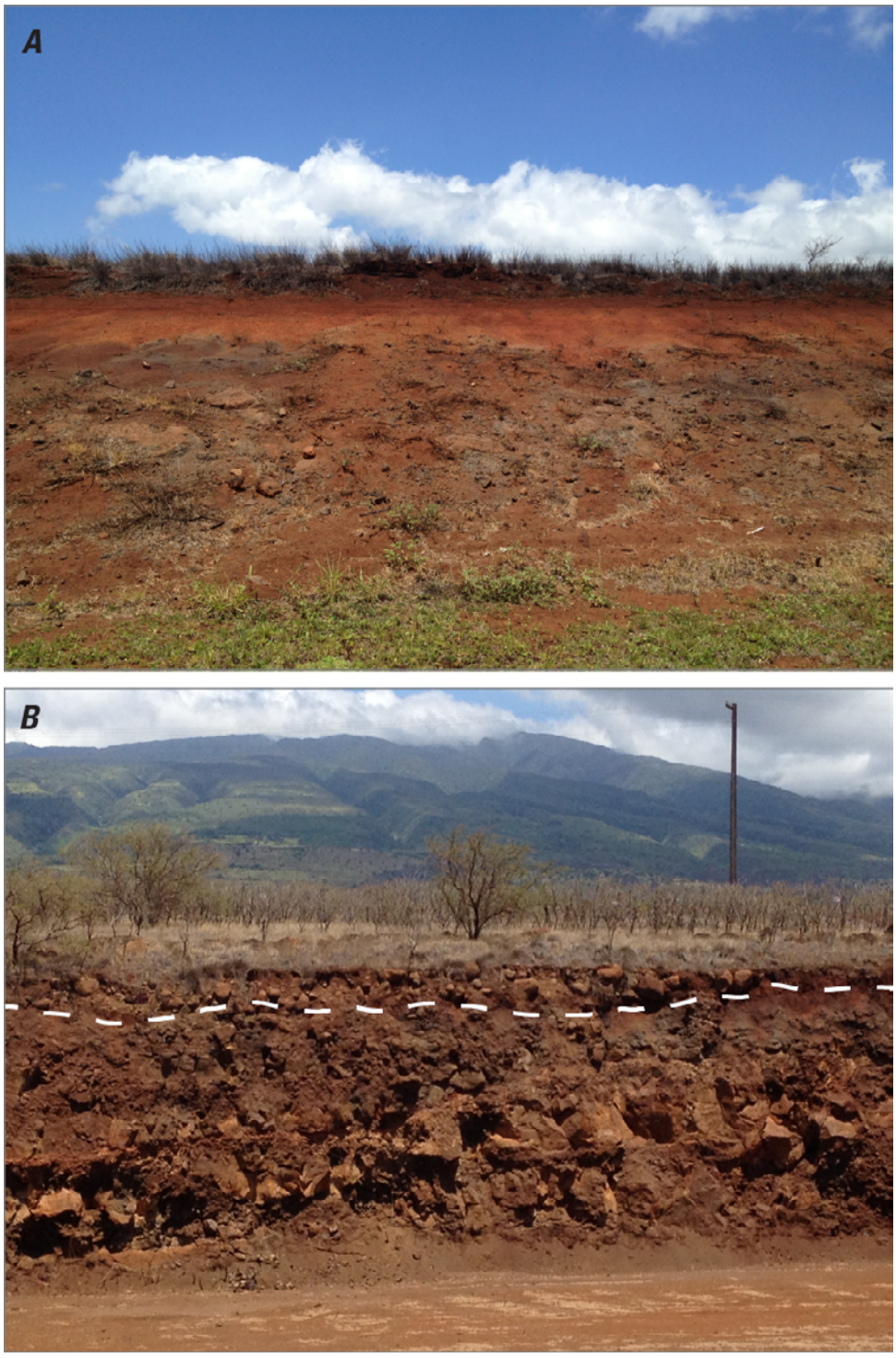

Figure 2. Photographs showing sediments overlying Honolua Volcanic flows. *A*, Fine-sand and silt deposits overlying Honolua Volcanic flows in the vicinity of Kaanapali Coffee Farms. These red to red-orange granular deposits, as much as several meters thick, are found on low-relief surfaces. They may represent volcanic air-fall deposits modified by pedogenesis or weathered saprolite modified by pedogenesis. The most intense coastal plumes are red to red orange in color, and may be sourced from deposits such as those pictured here. *B*, Quarry wall exposure of Honolua Volcanic flows capped by bouldery alluvium above dashed white line.

Geomorphic Processes in West Maui Watersheds

Closed-canopy forests cover the headwaters of West Maui watersheds (fig. 3*A*). Soils and saprolites throughout these landscapes are bound by dense root networks. Root activity, burrowing animals, tree throw (fig. 3*B*), and other episodic activity move soil incrementally downslope at rates that are proportional to local slope (see, for example, Gilbert, 1909; Roering and others, 1999). This slow, episodic downslope movement is called soil creep. Where soil-mantled slopes abut the channels, pockets of fine-grained, dark soil can be entrained by flows. These areas are locally disturbed by pigs rooting up the soil with their snouts and hooves (fig. 3*C*). More commonly, the margins of large valleys are so steep that soil is patchy or absent (fig. 3*D*). Where slopes begin to exceed friction angles equivalent to ~0.65 (herein all slopes are reported in radians), soils thin to patch exposures. At slopes greater than 0.70–0.85, soil cover over rock is uncommon. This exposed bedrock fails episodically as rockfalls, some of which mobilize into debris flows. These likely cut shallow valleys fluted into the main-valley sidewall (fig. 3*D*). This terrain produces coarse particles (gravel to boulders) from rockfall, landslides, and other mass-wasting processes. Boulders and other coarse products of rockfalls (fig. 3*E*) and small debris flows accumulate as talus aprons (fig. 3*F*) or cones at valley floor margins.

At elevations below closed-canopy forests, shrub- and grass-lands cover the planeze. In middle and lower watershed areas, these low-relief surfaces were modified to serve as agricultural fields for the production of sugar cane and pineapple. Since these practices ceased in the last decade, some fields have been developed as golf courses (for example, lower Honolua) or have been allowed to lie fallow (for example, lower Honokōwai). The episodic movement of soil by creep occurs under these different land covers, at rates that are not known.

Where human activity exposes soil or saprolite, rainfall rates influence transport. On slopes of exposed granular material, raindrop impacts send grains flying, with a net-downslope flux because those headed downslope travel farther than those moving upslope. This process of rainsplash leaves subtle pits in loose soil, particularly when the rainfall rates are too low to pond water. When rainfall rates exceed a soil's capacity to transmit water, ponded water may flow downslope as Horton Overland flow (fig. 4*A*), entraining and transporting granular materials. Where channelized, this flow leaves margins of loose vegetation fragments behind (grass, twigs, and leaves) and an interior washed clean of the loosest particles. Where subtle topography focuses this flow, rills (fig. 4*B*) and gullies form as water shear stresses entrain soil and saprolite. In developed land, drainage has been compartmentalized with local soil berms and water bars. Some flows travel into these unconfined areas and deposit sand and coarser particles in small depressions (fig. 4*C*). A few feed into tributary streams, providing a source of sediment-charged water to mainstream valleys.

Ancient alluvial-fan deposits of gravel, cobbles, and boulders can be found on the planeze. These deposits impede agricultural practice. Tool-marked boulders are now found in piles and as berms along the agricultural field margins. Piles of red-orange silty sand cascade over some field margins as sidecast (fig. 4*D*, *E*, *F*), the deposits formed by bulldozing material onto slopes.

Steep (slope >0.01) valleys of West Maui are floored by pool-riffle, plane-bed, step-pool, and cascade bedforms composed of gravel, cobbles, and boulders (for example, fig. 5*A*). Pebbles and coarse sand are present in protected pockets and probably represent the mode of bedload. Silt or clay films can be found in pools or stream margins or under large bed material. There are no obvious pavements or armor (coarse surface layers underlain by finer particles). Upstream-facing tree trunks have scars up to several meters above the present bed surface. Scar damage heights are level with some terrace tops. Most of West Maui's streams are (or were) floored with gravel or coarser material.

Terrace deposits have sedimentary textures which record deposition by debris flow, stream-traction transport, or overland flow. From headwaters down to valley slopes of 0.03–0.05, some terraces have unsorted mixtures of sand and pebbles as a matrix (fig. 5*B*). Gravel, cobbles, and boulders are either clast supported or floating in the matrix. These deposits lack imbrication and terrace surfaces commonly have aligned boulder berms. Silt and clay are likely present in the matrix but are not obvious in hand sample. These deposits record the passage of debris flows: mixtures of water, sediment, and vegetation flowing by inertia. By contrast, other terrace deposits are clast-supported layers of imbricated cobbles with sand and imbricated pebbles as matrix (fig. 5*C*). These deposits record the grain-by-grain deposition of particles moved by fluid traction. In headwater areas, higher terraces tend to be more weathered (in other words, older) than lower terraces. Downstream, the most weathered terraces are found by the margins of valley walls, and terraces closer to the active channel tend to be less weathered (in other words, younger).

Some valleys adjacent to agricultural fields have silty sand draped over prehistoric, coarser grained terraces (fig. 5*D*, *E*). These fine-grained deposits form historic terraces that at some places contain fragments of plastic irrigation drip line (fig. 5*F*) and other evidence of human agency. The deposits are locally connected to aprons of similar material that slope up to join agricultural fields, perhaps as alluvial fans formed by overland flow depositing sidecast.

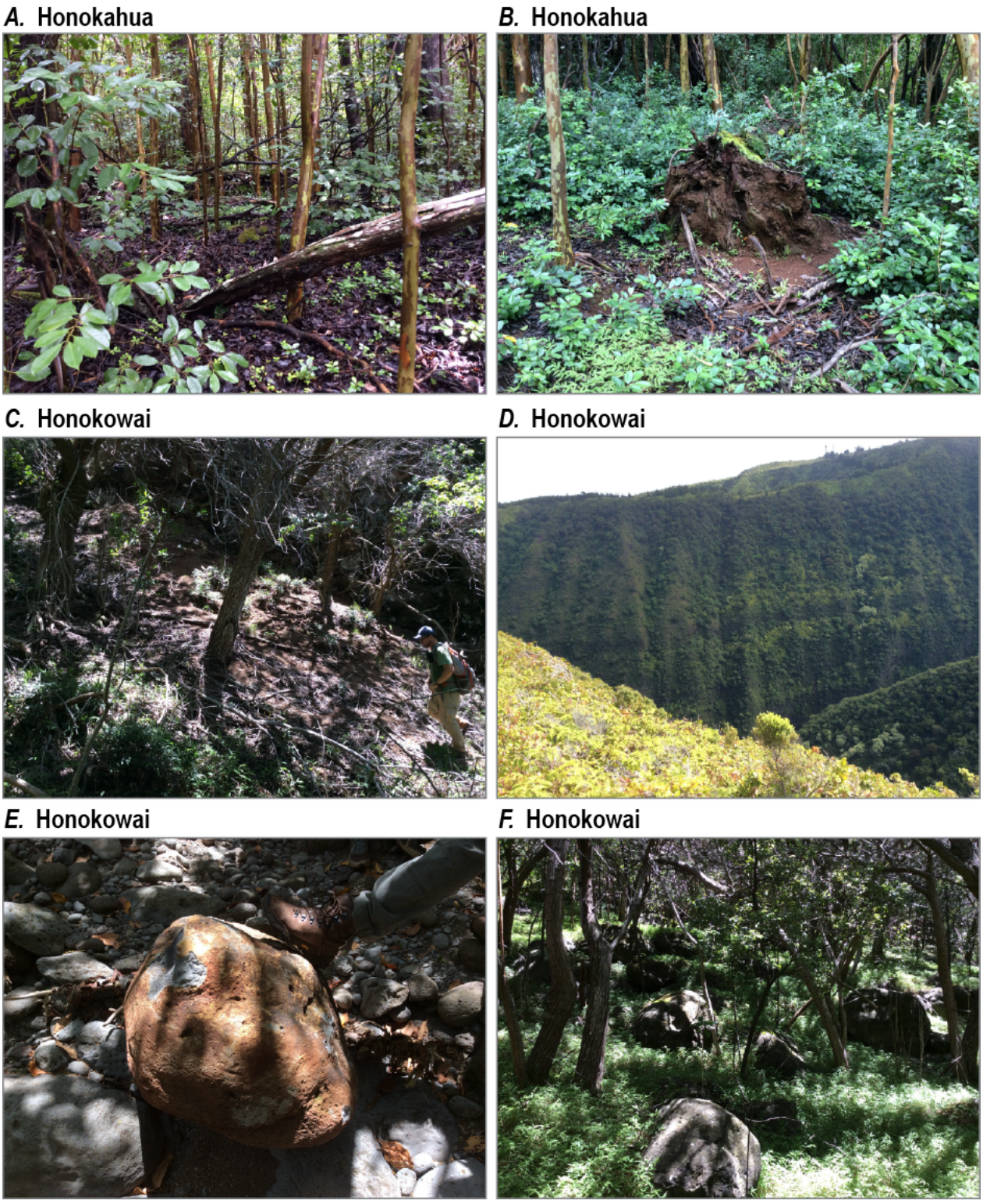

Figure 3. Photographs showing gravity-driven hillslope geomorphic processes of West Maui. *A*, Closed-canopy forests in headwaters, where sediment transport is characterized by slow, episodic soil creep. *B*, Example of soil creep from tree throw (episodic downslope soil movement from uprooted tree) in headwaters of Mokupe‘a valley. *C*, Soil-mantled slope abutting stream, with pig activity moving dark, organic-rich soil into channel to right. *D*, Hillslopes characterized by rockfall processes in Honokōwai watershed, north of Honokowai–upper rain gage. *E*, Weathered boulder showing impact marks from recent rockfall transport to Honokōwai streambed. *F*, Angular boulders deposited as talus by rockfall processes.

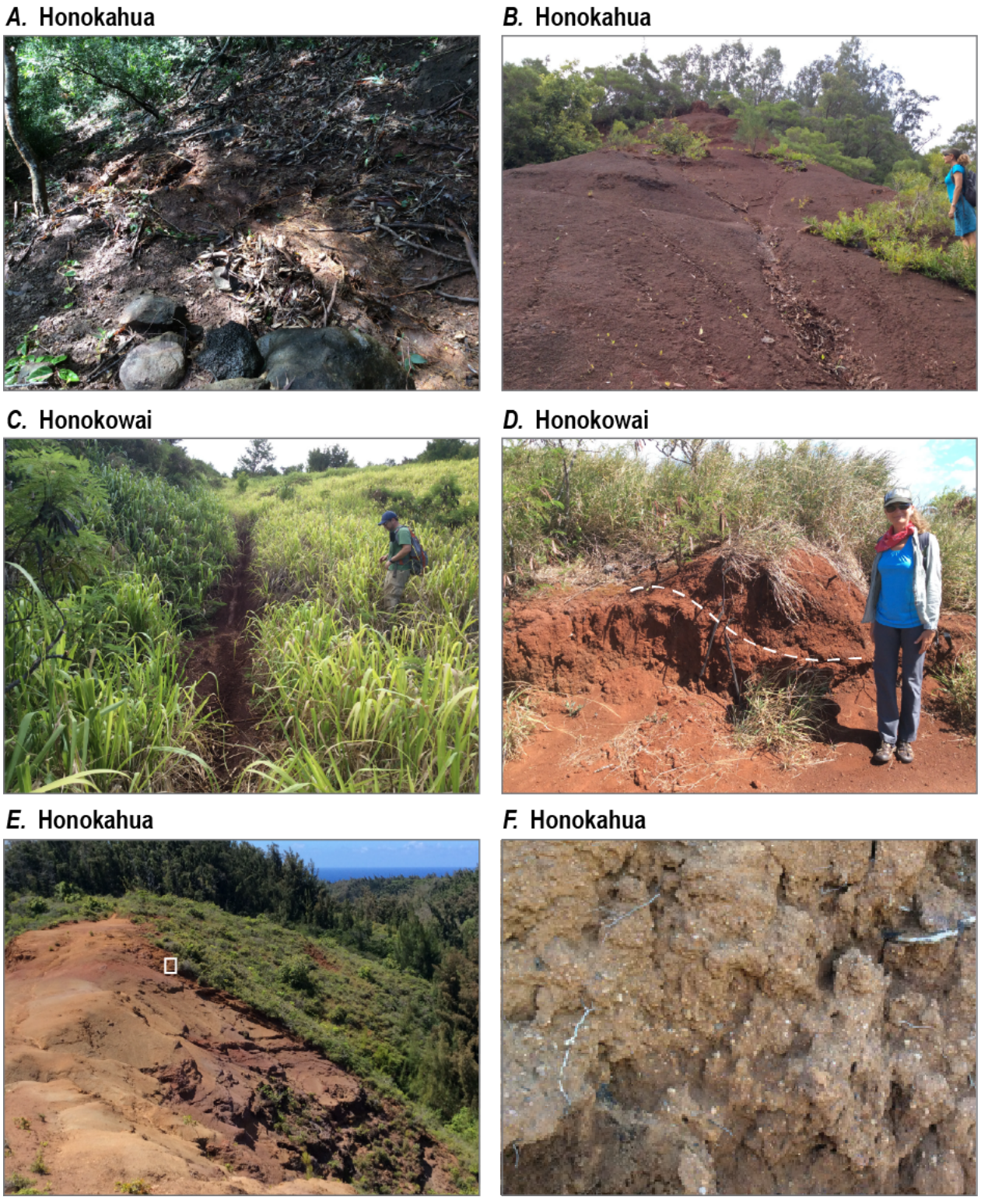

Figure 4. Photographs showing fluid-driven hillslope geomorphic processes in West Maui. A, Channelized Horton overland flow from July 19–20, 2014 rains. B, Horton overland flow focused into rills on exposed saprolite of Honolua Volcanics. C, Sediment deposited by Horton overland flow in water-bar area of former agricultural fields. D, Dashed line shows contact between fine sediments with plastic drip hoses, pushed over in-place soils with peds. E, Ridge between Honolua Stream and Pāpua Gulch, with sidecast layer removed by shallow landsliding and overland flow. Remnants of sidecast form an apron thinning downslope, delineated by dark, shadowed scarp running from center left of image to lower right. White box shows location of F. F, Close-up of sidecast, illustrating non-sorted deposit with fragments of burned shrubs concentrated near its base.

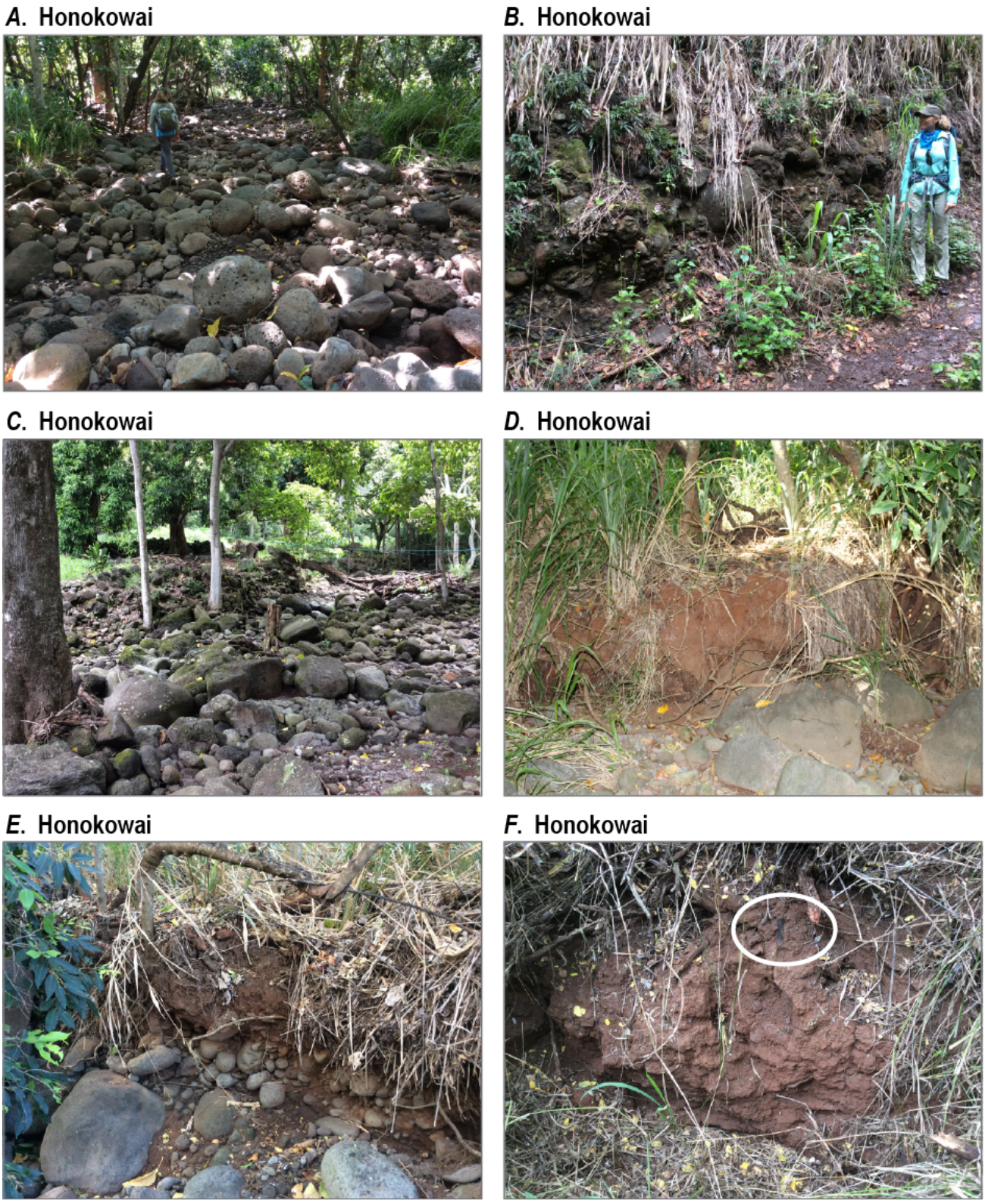

Figure 5. Photographs showing valley geomorphic processes in West Maui. *A*, Gravel-bedded stream typical of fluvial sediment transport down slopes of 0.01–0.08 in valleys of West Maui. *B*, Unsorted, unimbricated terrace sediments likely deposited by debris flows, mobile at slopes greater than about 0.03–0.05. *C*, Sorted, imbricated deposits of a fluvial terrace, above dashed white line. *D*, Fine sands, silts, and clays deposited as a historic fill terrace above Honokōwai sediment impoundment basin. *E*, Anomalous terrace of fine sediments overlying gravel deposits that are characteristic of West Maui's gravel-bedded streams with slopes of 0.01–0.08. *F*, Historic fill terrace, upstream of *D*, with embedded plastic drip hose from field-irrigation system (white circle).

Methods

Infiltration and Particle-Size Analysis

To estimate rainfall rates that would cause overland flow on exposed soils, we performed 13 tension-disc infiltrometer measurements at 6 areas in former agricultural fields and unimproved roads (fig. 6), mostly on Hawaii State lands. These two land uses account for much of the exposed soil in West Maui that could provide fine sediment from hillslope runoff. At each measurement site (for example, fig. 7*A*, *B*), we chose a representative patch of undisturbed soil, cleared vegetation, or large rock fragments from the surface, and used Decagon's tension disc infiltrometer to infiltrate water. We varied suction heads from −1 cm to −5 cm to achieve a 15–30-minute-long infiltration test. After each test, we excavated pits to look at subsurface water distribution. The patterns were elongated half spheres in cross section, consistent with the absence of strong preferred flow paths in the well-mixed, fine-sandy soils. We sampled soil from each site to characterize particle-size distribution, and used the resulting U.S. Department of Agriculture (USDA) soil classification to estimate the van Genuchten parameters (van Genuchten, 1980) using Decagon's manual. From these tests, we calculated the saturated hydraulic conductivity (K_{sat}) of the soils as an approximation of the rainfall rate above which soils would begin to pond water and erode by overland flow. The recurrence interval of storms that exceed this threshold rainfall rate should provide an estimate of how often agricultural fields could release sediment to the nearshore.

We used a Beckman Coulter laser diffraction particle analyzer to measure grain-size distributions of soils. We did not pretreat or sonicate soils to disaggregate them. Consequently, the grain-size distributions that we report represent the distribution of particle sizes relevant to permeability or sediment transport, not the grain-component mineralogy owing to weathering.

Rainfall Analysis

We searched the National Weather Service rainfall database for gages with 15-minute recording intervals near Honolua and Honokōwai watersheds (National Oceanic and Atmospheric Administration, 2014). We used this subhourly data to understand the historic record of rainfalls intense enough to cause erosion, their recurrence interval, and the intensity distribution of rainfalls for historic storms. The intent was to understand how often rainfalls could cause soil erosion and whether that frequency is changing. We used four gages (fig. 6, table 1) whose records span 7.3 to 27.6 years. Three of the gages are in the uplands where trade-wind-driven rainfalls are present (Field 46, Field 28, and Puu Kolii) and one gage is at the coast (Lahaina) where rainfall is dominated by low-pressure cyclonal events (for example, Kona storms) or episodic frontal systems. Median rainfalls at the gages are ~200 millimeters per year (mm/a) at arid, coastal Lahaina and increase to the north from ~400 mm (Puu Kolii) to ~1,700 mm (Field 46).

We removed a few spurious rainfall entries from the source data (for example, an isolated entry of 0.81 inches in 15 minutes). Each gage has missing data (table 1). Annual totals are summed over each water year, which starts on October 1 of each calendar year. The gages record rainfall at 2.54 mm intervals, so data are not continuous. We calculated rainfall intensity over 1- and 2-hour periods using backward differencing (in other words the intensity represents the total rain that fell over the past 1–2 hour period). We used the data to create graphs of the number of hours each water year that 15-minute rainfalls exceeded thresholds from 20 to 50 mm/hr and the recurrence interval for 1- and 2-hour rainfall intensities from 20 to 50 mm/hr. We calculated recurrence interval τ_r as follows (table 2):

$$\tau_r = (n_{present} - n_{missing} + 1)/\text{rank} \quad (1)$$

where

$n_{present}$ is the hours of rainfall present in the total record, and

$n_{missing}$ is the hours of rainfall missing from the total record.

Events are ranked in order of decreasing intensity, so that the largest rainfall intensity has a rank of 1, with rank increasing to $n_{present}$, the total number of rainfall hours in the record. In graphs, τ_r is expressed in years.

To characterize the distribution of rainfall intensities in a given storm, we plotted the total number of hours exceeding a given intensity versus the intensity value. These plots are a convenient way to characterize both rain intensity and amount with two parameters. Once the saturated hydraulic conductivity (K_{sat}) of a surface is known, the plot can be used to estimate the hours of runoff and erosion that a storm could cause by reading the hours exceeded at a given conductivity.

Finally, we used the gages to reconstruct a history of heavy rainfall events in West Maui, as conveyed by the number of hours of continuous rainfall at intensities greater than 20–40 mm/hr. These records provide a sense of past storms capable of causing large sediment plumes in the near shore.

Geomorphic Mapping

We used 10-m USGS topography and 2013 1-m DigitalGlobe imagery to map geomorphic processes in Honolua and Honokōwai watersheds and some surrounding areas. We derived slope maps of the 10-m topography using the maximum fall algorithm in ArcGIS, and we extracted a valley network by filling sinks and extracting drainage areas larger than 20,000 m^2. We have found that including drainage area values below this threshold can sometimes lead to artifactual valley networks. The crude nature of the 10-m data, compared to 1-m lidar, means that many smaller features cannot be resolved and are absent from the map (for example, landslide deposits, talus, terraces, and valley-margin details).

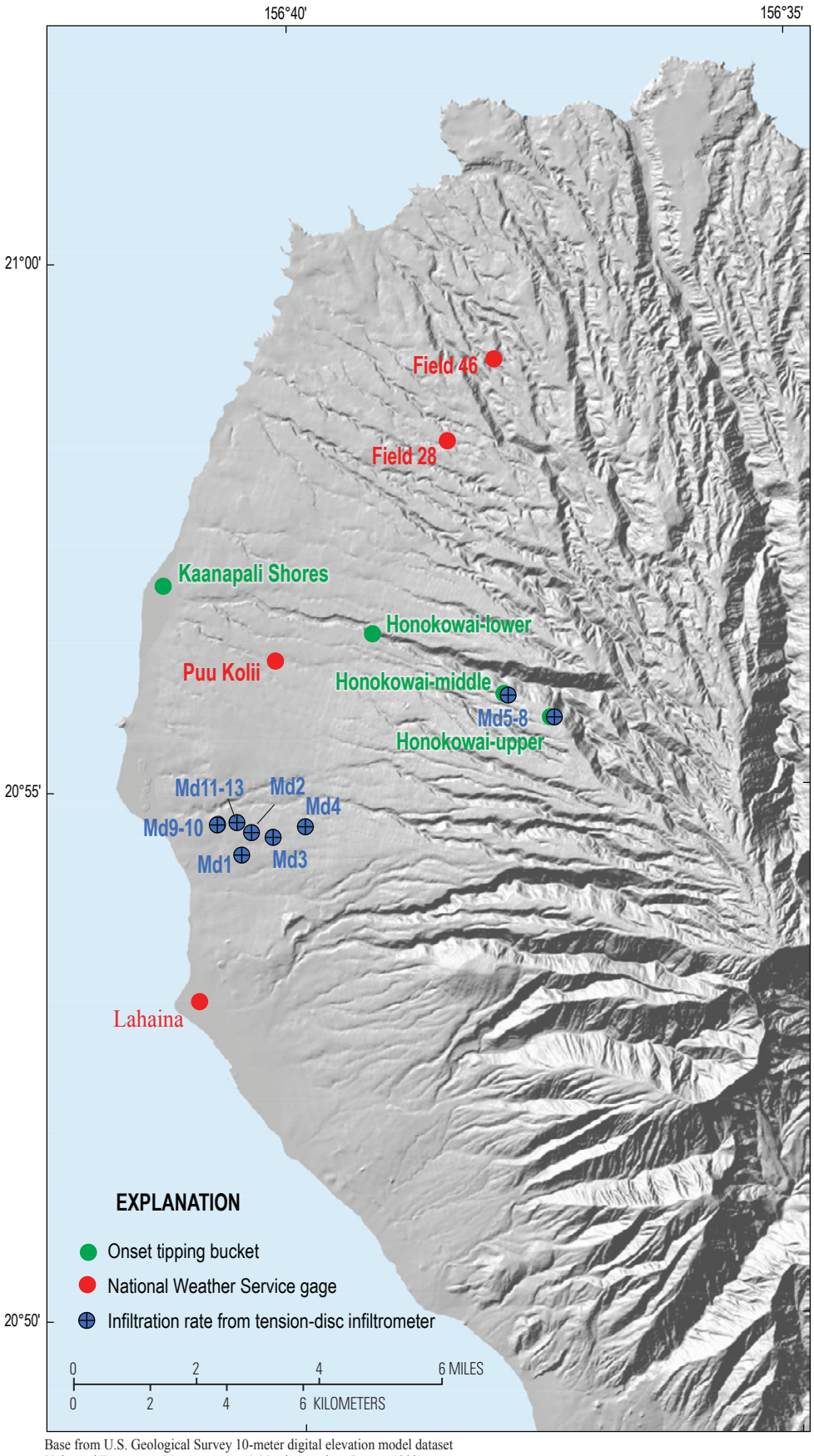

Base from U.S. Geological Survey 10-meter digital elevation model dataset
Universal Transverse Mercator, zone 4, North American Datum 1983

Figure 6. Map showing locations of rain gages and infiltration test sites on West Maui. National Weather Service gage data was obtained from National Oceanic and Atmospheric Administration (2014). Onset RG3M tipping bucket rain gages were installed in spring of 2014 by Tova Callender. Infiltration rates were determined from 13 infiltration tests conducted at 6 general sites with a tension-disc infiltrometer.

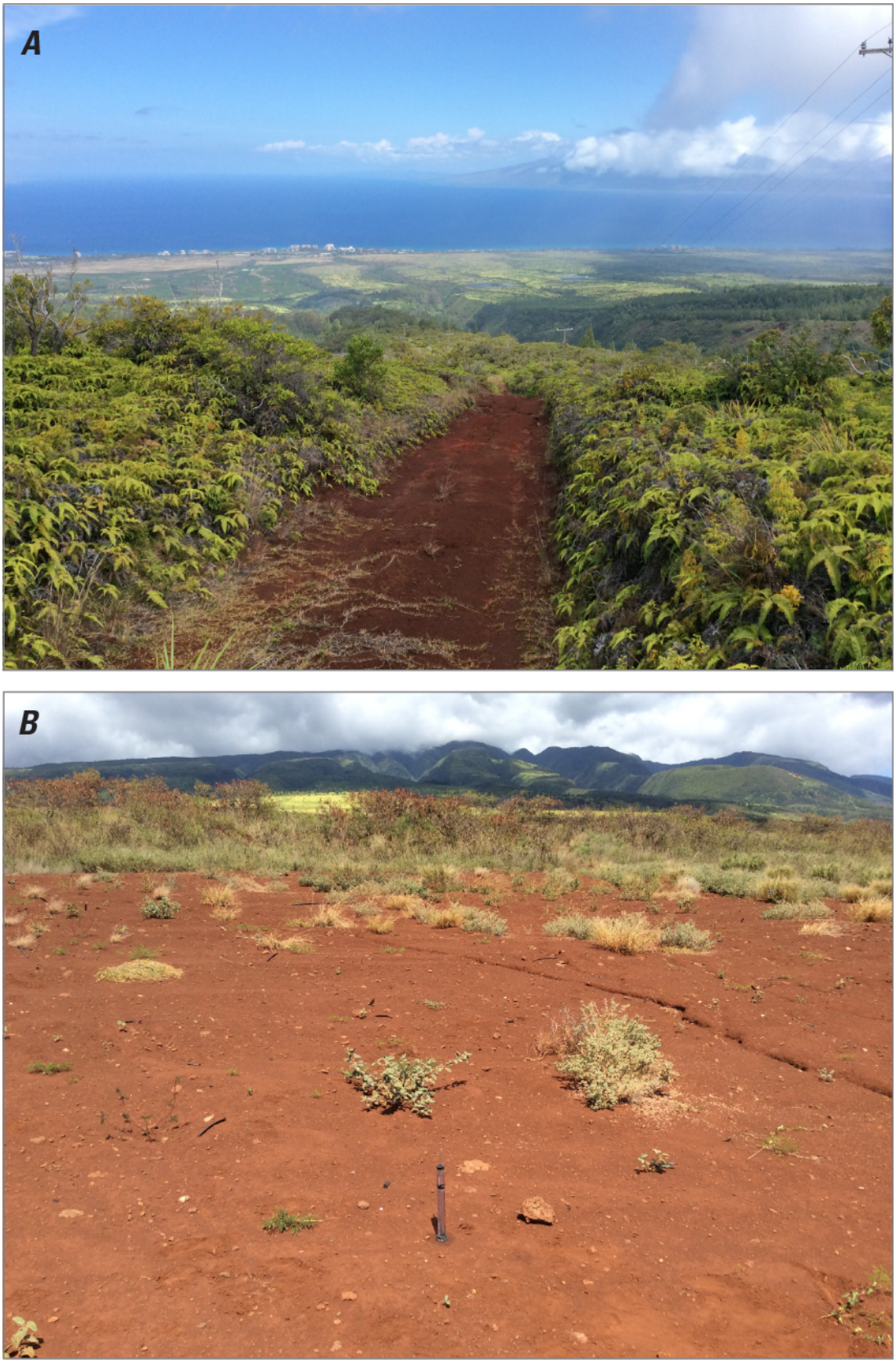

Figure 7. Photographs showing examples of infiltration-test sites at locations in figure 6. A, Unimproved road south of Honokōwai Stream with evidence of minor runoff from July 19–20, 2014 rainfalls. We conducted hydraulic conductivity tests Md 5–8 along this road. B, Trace evidence for road runoff on former agricultural fields south of Wahikuli Gulch; site of Md 9–10 hydraulic conductivity tests.

Table 1. Characteristics of selected National Weather Service listed rain gages, West Maui.

[m, meters; mm/hr, millimeters per hour; mm/a, millimeters per year]

Site	Elevation (m)	Median rain (mm/a)	Mean rain (mm/a)	Heavy rain[1]	Very heavy rain[2]	Sustained heavy rain[3]	Start date	End date	Record (years)	Missing data (years)
Lahaina	5	239	275	3.0	0.7	0.8	11/1/1977	10/25/2001	24.0	0.036
Puu Kolii	46	443	460	5.6	1.6	1.1	7/1/2002	4/1/2013	10.8	0.009
Field 28	107	1,055	1,017	7	2	1.4	1/5/2006	4/19/2013	7.3	0.021
Field 46	98	1,725	1,809	12.8	3.1	2.0	3/1/1978	10/14/2005	27.6	0.015

[1]Hours per year with rainfall intensity >20 mm/hr

[2]Hours per year with rainfall intensity >40 mm/hr

[3]Continuous hours per with year rainfall intensity >20 mm/hr

Table 2. Recurrence intervals for exceedance rainfalls.

[mm/hr, millimeters per hour]

Rainfall intensity exceeds (mm/hr)	Field 46		Lahaina	
	1-hour recurrence (years)	2-hour recurrence (years)	1-hour recurrence (years)	2-hour recurrence (years)
20	0.2	1.6	0.6	2.7
30	0.4	3.9	3.5	24.0
40	0.8	> 27.6	6.0	>24.0
50	1.5	>27.6	12.0	>24.0
60	3.1	>27.6	>24.0	>24.0
70	4.6	>27.6	>24.0	>24.0

We divided the watershed area into rockfall, soil creep under canopy, soil creep without canopy (shrub and grasslands), overland flow (exposed soils), valley deposits, terrace deposits, and talus. To map rockfall areas, we used DigitalGlobe imagery and topographic slope to find steep (typically slope >0.65) valley walls with thin to absent soil and exposed bedrock (see, for example, fig. 3*D*). Small valleys sometimes indent or flute these rock walls. We mapped the extent of soil creep (for example, fig. 3*A*, *B*, *C*) using 2014 DigitalGlobe imagery to identify areas of canopied forest (excluding rockfall areas), grasslands, and fallow fields.

Talus occurs as aprons of boulders (for example, fig. 3*E*) below rockfall areas and can be identified in DigitalGlobe imagery by the presence of accumulated boulders deposited on slopes below rockfall areas (for example, fig. 3*F*). We mapped large landslides using the presence of headscarps, lateral scarps, and displaced masses evident on the 10-m topography (features tens to hundreds of meters in dimension). With one exception, they have the same canopy cover as adjacent areas, indicating that they are likely prehistoric.

We used low-slope areas of the valley bottom to delineate the extent of valley deposits that characterize the debris-flow and fluvial-transport system (see, for example, fig. 5*A*). We identified prominent terraces by mapping the boundaries of steep-walled benches adjacent to valley deposits. These features are typically more than 3-m-high accumulations of fluvial or debris-flow deposits. Many smaller benches are not resolved by 10-m data and are included in the valley deposits unit (see, for example, the terraces in fig. 5*B*, *C*).

We used 1-m DigitalGlobe imagery to map features that are consequences of human modifications to the landscape, such as displaced colluvium and coalesced landslides. Displaced colluvium results from machine-moved soil, vegetation, and boulders piled in field centers or margins as push piles (fig. 4*D*) or pushed off of the margins of the fields or roadways as sidecast (fig. 4*E*, *F*). Freshly exposed soil and rock occur on some ridgelines in Honolua and other watersheds. These exposures, locally, have headscarps and lateral scarps in soils, indicating that the processes maintaining fresh exposure are a combination of overland flow erosion and shallow landsliding.

Reconnaissance Sediment Budget

To construct a reconnaissance budget for suspended sediment, we summed up the areas of each geomorphic process in a watershed, and multiplied each of the totals by a notional lowering rate and a soil bulk density. This yields the expected annual suspended-sediment flux in metric tons per year. This is a reconnaissance budget because there are no known sediment yields or erosion-monitoring data for the watersheds of West Maui; instead, we use erosion-rate estimates based on work elsewhere in the Hawaiian Islands. For instance, rockfall and soil creep erode sediment in large fractions of watershed areas. Erosion rates from these processes are not known in West Maui. Below we explore the logic for estimating their rates, and test this against measured sediment yields from the least disturbed Hawaiian watersheds.

For undisturbed watersheds, the vertical component of the lowering rate of valley sidewalls should approach the long-term valley incision rate, the boundary condition for hillslope processes (in other words, the boundary lowering rate). We calculated valley-lowering rate midway up the basin, dividing valley relief by the age of the uppermost volcanic deposit: 1.1–1.3 Ma (Sherrod and others, 2007). In the Honolua watershed, in the vicinity of Mahana (fig. 1), this calculation is ~128 m/(1.1 to 1.3 Ma), yielding a long-term bedrock valley lowering rate of 0.09–0.11 mm/a.

Rockfall produces a small fraction of suspended-sediment-sized particles. Because talus deposits are clast supported, porosities of around 30 percent represent the upper bound to this fraction, although the value is likely much smaller. So, in areas of rockfall, the component of lowering that contributes suspended sediment is likely to be much less than the overall boundary lowering rate of 0.09–0.11 mm/a. One can calculate a maximum bound by assuming that 30 percent of the lowering contributes to pore-filling particles such as sand and silt. This would yield a lowering rate of about a third of the valley lowering rate of ~0.1 mm/a, or ~0.03 mm/a. We multiply the area of rockfall processes by this value to model the expected annual suspended-sediment load from rockfall. The true value is likely to be closer to 0.01 mm/a because it is unlikely that a third of rockfall by volume produces fine sediment.

Low-relief surfaces far above the valley floor record minor lowering following deposition as lava flows or capping air falls. Their lowering rate is likely several orders of magnitude less than a valley boundary-lowering rate. Small first-order valleys are cut less than ~10 m into these surfaces at Honolua and Honokōwai watersheds. This suggests that over the 1.1–1.3 million years since deposition, rock-lowering rates were, very crudely, 10 m/(1.1–1.3 Ma), or 0.01 mm/a. The equivalent soil lowering rate would be 0.03 mm/a for a ratio of bedrock to soil bulk density of 2,900/950 kg/m^3. If small-valley lowering rates were an order of magnitude greater than 0.01 mm/a in these areas, these surfaces would not have endured. Multiplying a crude estimate of a lowering rate of 0.01 mm/a by soil creep area yields a notional annual suspended-sediment flux for long-term soil creep rates.

Former agricultural fields were developed on low-relief surfaces. Their vegetation cover has been modified by many decades of land use. Where they expose large areas of sands and silts, they represent the largest apparent reservoir of suspendable sediment in West Maui. We have no constraints on their lowering rates under current conditions. The absence of valley incision into these surfaces over the last 1.1–1.3 Ma suggests long-term lowering rates approach 0.01 mm/a or less. Industrial agriculture over historic time certainly increased these values by episodically removing vegetation. For the purposes of exploring effects on the sediment budget, we estimate loads from these sources using lowering rates representing 10–100 times the long-term rate, or 0.1–1 mm/a.

Both talus and prehistoric terrace deposits represent potential sinks for fine sediment, so we assume that their contribution to the sediment budget is negligible. Valley deposits are primarily gravel deposits of the active streams and terraces that are not imaged by coarse topographic data. Both elements could be storage sites for fine sediment originating from rockfall, soil creep, and overland flow areas. For instance, field observations indicate that fine sands, silts, and clays are in the matrix between gravel clasts of active streams. These fine sediments would be released when gravel moves. Bank erosion of historic valley terraces is also a source of suspended sediment. We calculated this value by summing up a valley network length likely to have fine-grained historic terrace deposits, doubling it to account for both banks, and then arbitrarily choosing a bank-exposure value (10 or 50 percent exposed) and a lateral erosion rate (1, 10, and 100 mm/a). Monitoring of bank erosion at Kawela Gulch on Moloka‘i for 5 years indicates surface-normal lowering rates of ~10–100 mm/a for fine-grained sediment (J. Stock, unpub. data).

Results

Observations Following the Rainfalls of July 19–20, 2014

A cyclonal storm generated rainfall on West Maui, beginning 16:30 HST July 19, 2014, and ending 14:10 HST on July 20 (herein all times of day are HST). Maximum intensities occurred from about 06:00 to 08:00 on July 20. Tipping-bucket gages recorded rainfall totals of 67 mm at Honokowai-upper, 80 mm at Honokowai-lower, and 23 mm at Kaanapali Shores (fig. 8*A*). The gages recorded rainfall for a total of 14–15 hours at intensities that were mostly less than 20 mm/hr (fig. 8*B*). Rainfall records here show an exponential pattern of rainfall hours above a given threshold (fig. 9), a pattern that we have also found on Moloka‘i.

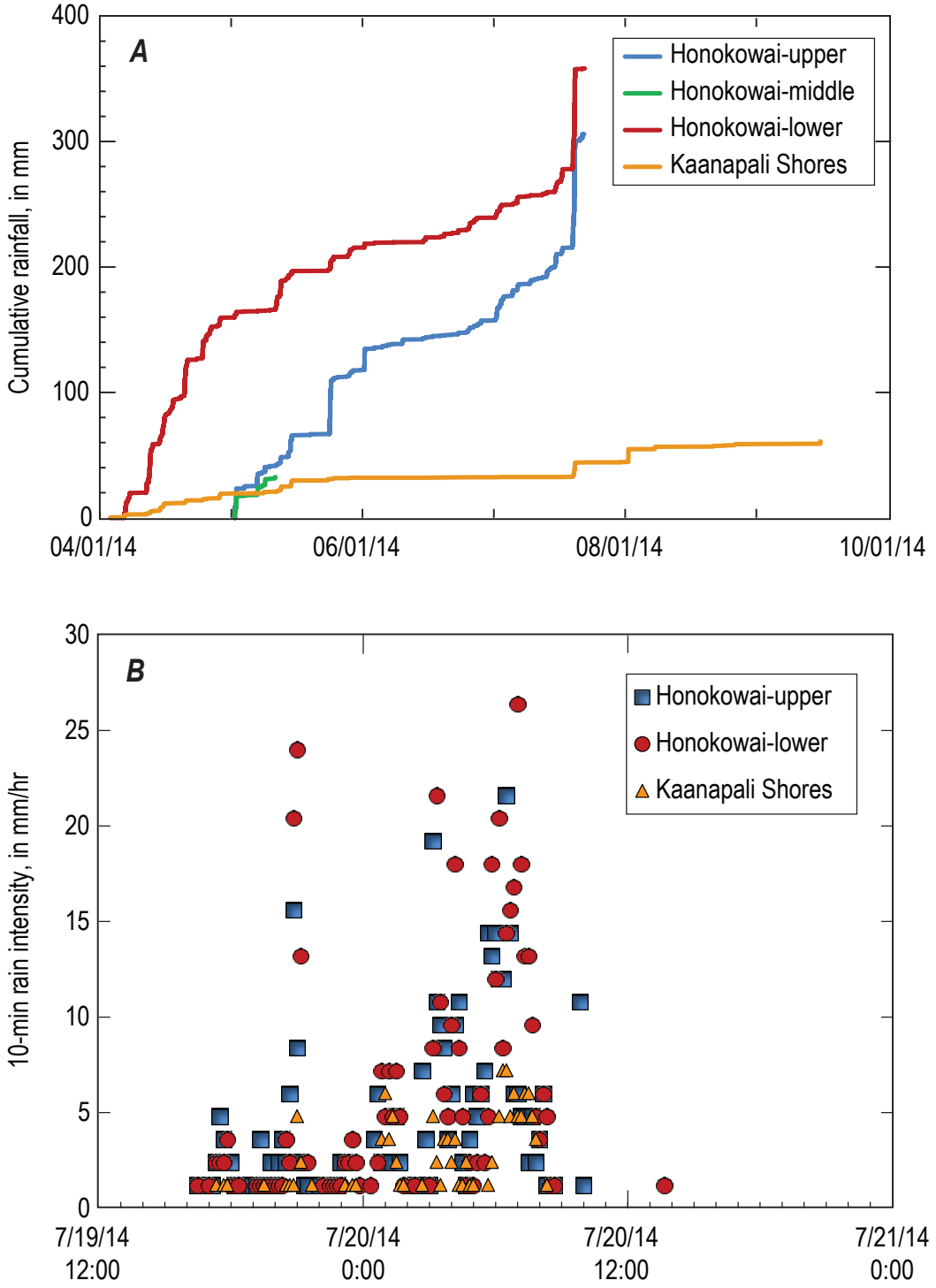

Figure 8. Plots of West Maui rainfall. *A*, Cumulative rainfalls for West Maui gages at locations shown in figure 6. These Onset RG3m tipping bucket rain gages were installed in spring of 2014 by Tova Callender. Data loss abbreviates the Honokowai-middle record. Rainfall totals for July 19–20, 2014, were roughly equivalent for the non-coastal gages (Honokowai-upper was 67 mm [millimeters], Honokowai-lower was 80 mm) and much less at Kaanapali Shores on the coast (23 mm). *B*, Rainfall intensities at 10-minute discretization recorded by tipping bucket gages during the storm of July 19–20, 2014. The upper two gages peak at intensities of about 25 mm/hr (millimeters per hour). The coastal gage intensities did not exceed 10 mm/hr. Rainfalls of 10–25 mm/hr at non-coastal gages occurred from 06:00 to 08:00 HST, triggering coastal plumes.

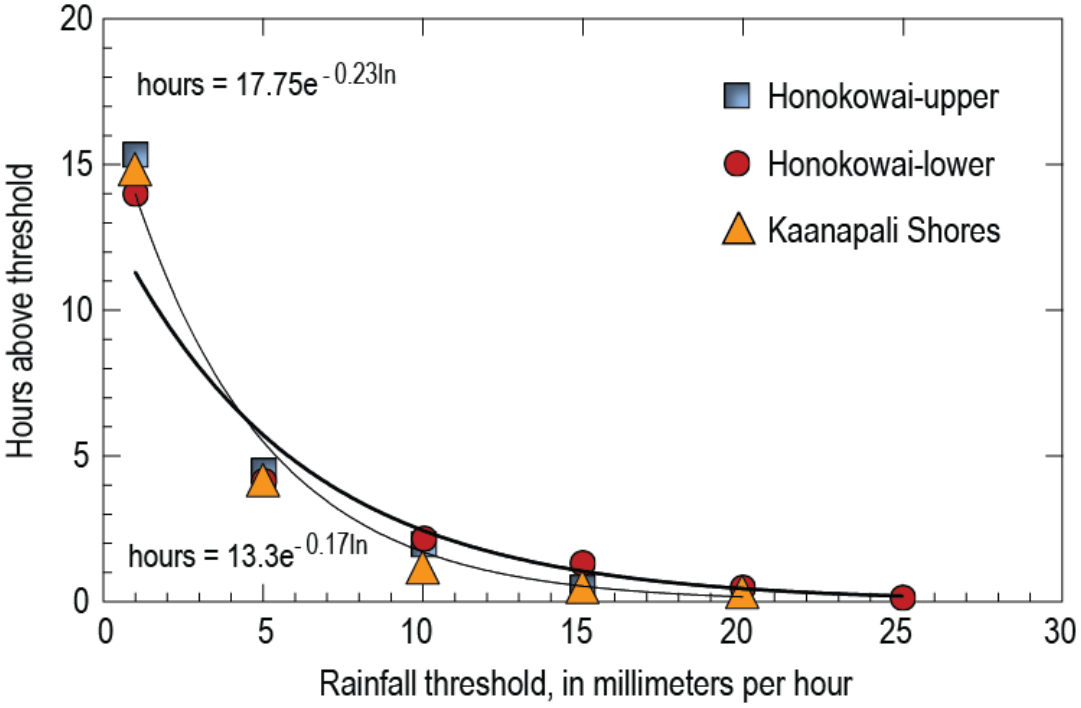

Figure 9. Plot showing cumulative exceedance rainfall intensities for tipping bucket gages. Data can be approximated by an exponential function with two parameters. Coastal rain gage at Kaanapali Shores has lower rainfall intensities, which lower its rainfall total. The two-parameter exponential function is useful to characterize rainfalls, illustrating hours of likely runoff if the saturated hydraulic conductivity of a surface is known. Curves are fitted to Honokowai-lower (lower equation) and Honokowai-upper (upper equation).

Rainfalls during the night of July 19 and morning of July 20 resulted in sediment plumes at the mouths of many West Maui streams (figs. 10–13). Beginning at 13:10 on July 20, about 5–6 hours after the most intense rainfalls, the first author visited all discharging streams (figs. 12, 13). The color and intensity of the sediment plumes varied from low-intensity brown-tea colors in northernmost drainages, growing progressively more red orange towards Ka‘ōpala, and turning brownish at Honokōwai. These plumes were generated by low-intensity rainfalls on the night of July 19, with peak intensities approaching 10–20 mm/hr for over 40 minutes.

Rainfalls of July 19–20 did not produce widespread overland flow in fields or roads (see, for example, fig. 7). In the fields, we observed evidence of patches of roadway runoff that produced flow, which then dissipated in the fields. We did not observe any unconfined flow, rills, or gullies moving water from former fields to channels. Unimproved roads cross the low-relief planeze of West Maui. Some have runoff-limiting structures such as water bars (fig. 4*C*). Road surfaces are composed of red-orange air-fall deposits of varying compaction. Long-occupied roads such as the Honokōwai ridge road in figure 7*A* have compacted down to dense layers. These surfaces generated runoff during the July 19–20 storm, and we observed local accumulations of sediment in ponded areas. We did not see any of these roadways dumping sediment and water into streams, but that is possible.

There are abandoned trails and roadways along ridges and on planeze margins. Some watersheds contain a network of active dirt-bike trails on ridges and along streams. Trail and roadway features are distinguished by bare surfaces, which can be incised meters below original A-horizon soils. Bare patches on the margins of these features record erosion by concentrated flow (fig. 4*B*) or shallow landslides. In some cases, the landslides appear to occur in old-road sidecast made of non-sorted colluvium with burnt vegetation fragments (for example, fig. 4*E*, *F*).

The agricultural ditch system that brings water from within the Honolua watershed to the Wahikuli watershed was observed to be eroding where the ditch system was unlined. After Wahikuli Reservoir was decommissioned and breached in 2013, the remaining water in the system is now delivered to Wahikuli and Honokōwai Streams. Ditch water creates flow in streams that is not directly correlated with rainfall events.

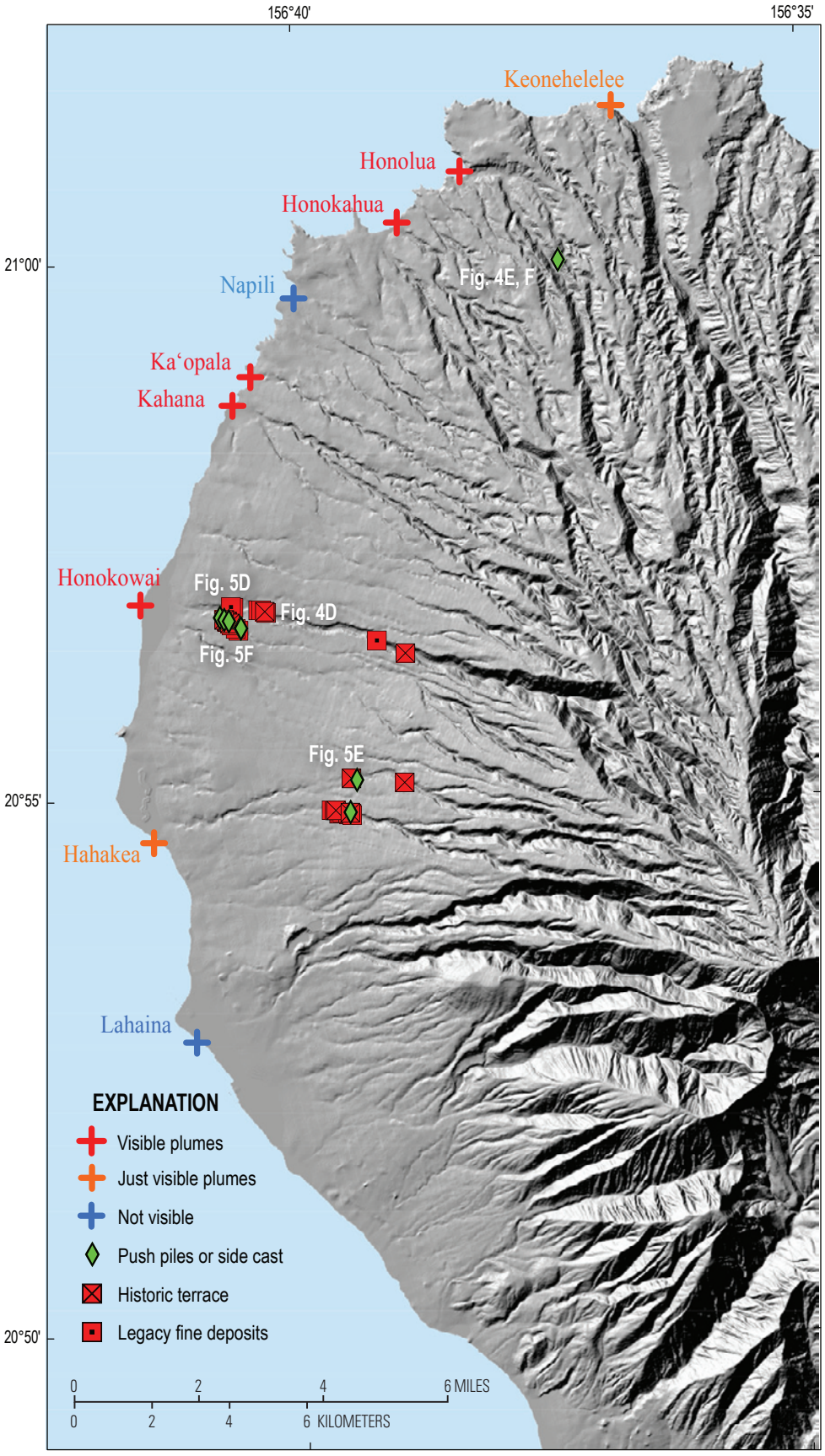

Base from U.S. Geological Survey 10-meter digital elevation model dataset
Universal Transverse Mercator, zone 4, North American Datum 1983

Figure 10. Map showing locations of coastal plumes observed July 20, 2014, 13:00–18:00 HST. Intense rainfalls occurred from about 06:00 to 08:00 (fig. 8*B*), 5–7 hours prior to the beginning of these observations. The most turbid runoff occurred south of Honolua and north of Honokōwai. Nāpili Bay lacked a plume because the turbid stream draining into it lacked sufficient discharge to breach a blocking sand berm. Push piles and side cast are composed of fine sediment. Historic terraces are composed of silt and fine sand. There are numerous near-stream sources of fine sediment that may generate coastal plumes at low stream flow.

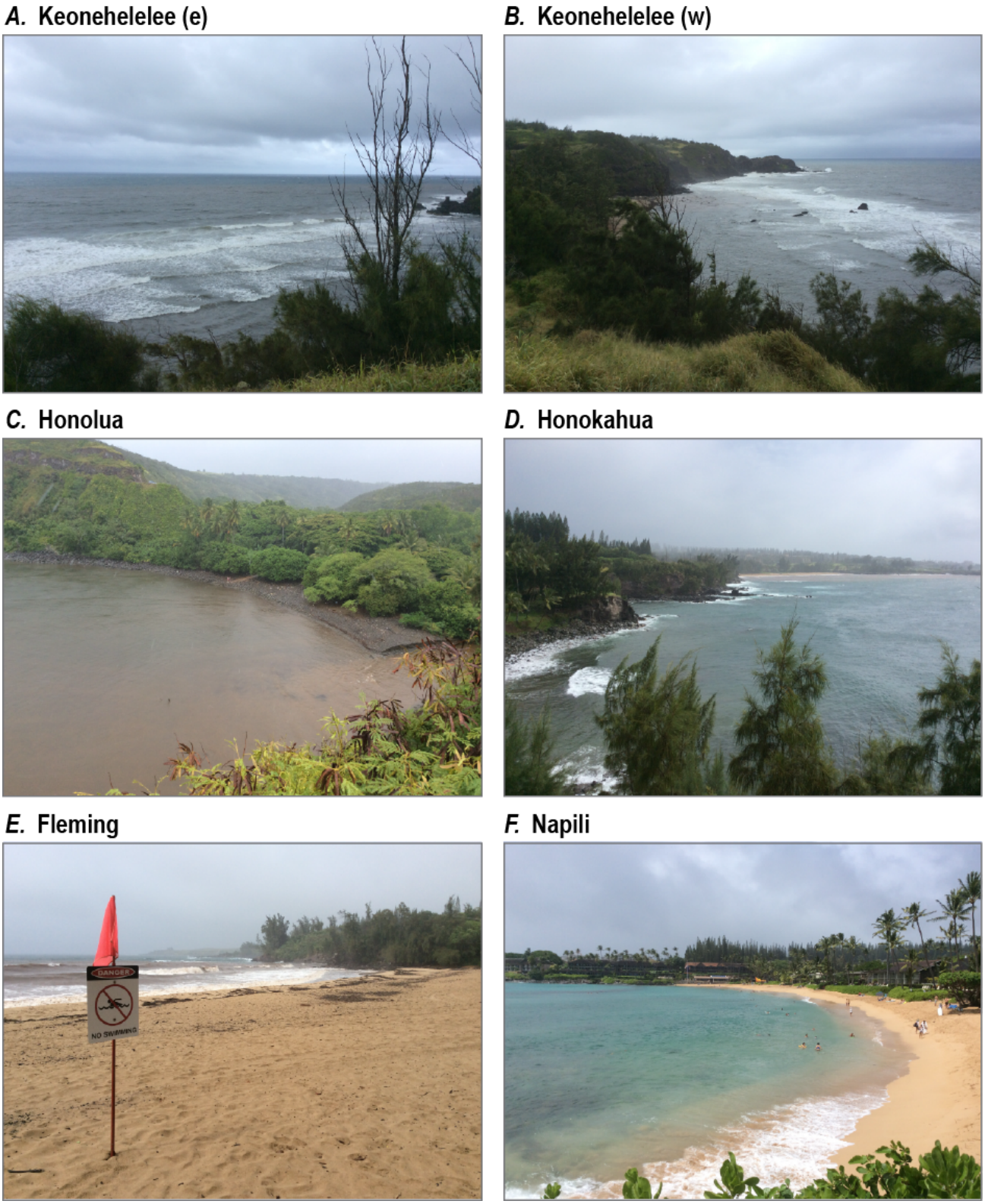

Figure 11. Photographs of West Maui coastal plumes (from north to south) observed July 20, 2014, 13:00–18:00 HST (*A*–*K*) and July 30 (*L*). *A*, Looking east (e) of Keonehelelee; plume is defined by a water color difference near horizon. *B*, Looking west (w) of Keonehelelee; no obvious plume. *C*, Honolua Bay, plume at stream mouth as muddy water. *D*, Honokahua Bay; plume in distance. *E*, D T Fleming Beach Park. *F*, Nāpili Bay; no plume. *G*, Kaʻōpala outlet looking north (n). *H*, Kaʻōpala outlet looking south (s). *I*, Kaʻea Point looking north. *J*, Kahana Stream outlet. *K*, Honokōwai Stream outlet. *L*, Looking south from Honokōwai, showing sediment plume remaining 10 days after July 19–20 event.

G. Ka‘opala (n)

H. Ka‘opala (s)

I. Ka‘ea

J. Kahana

K. Honokowai

L. Honokowai (s)

Figure 11.—Continued

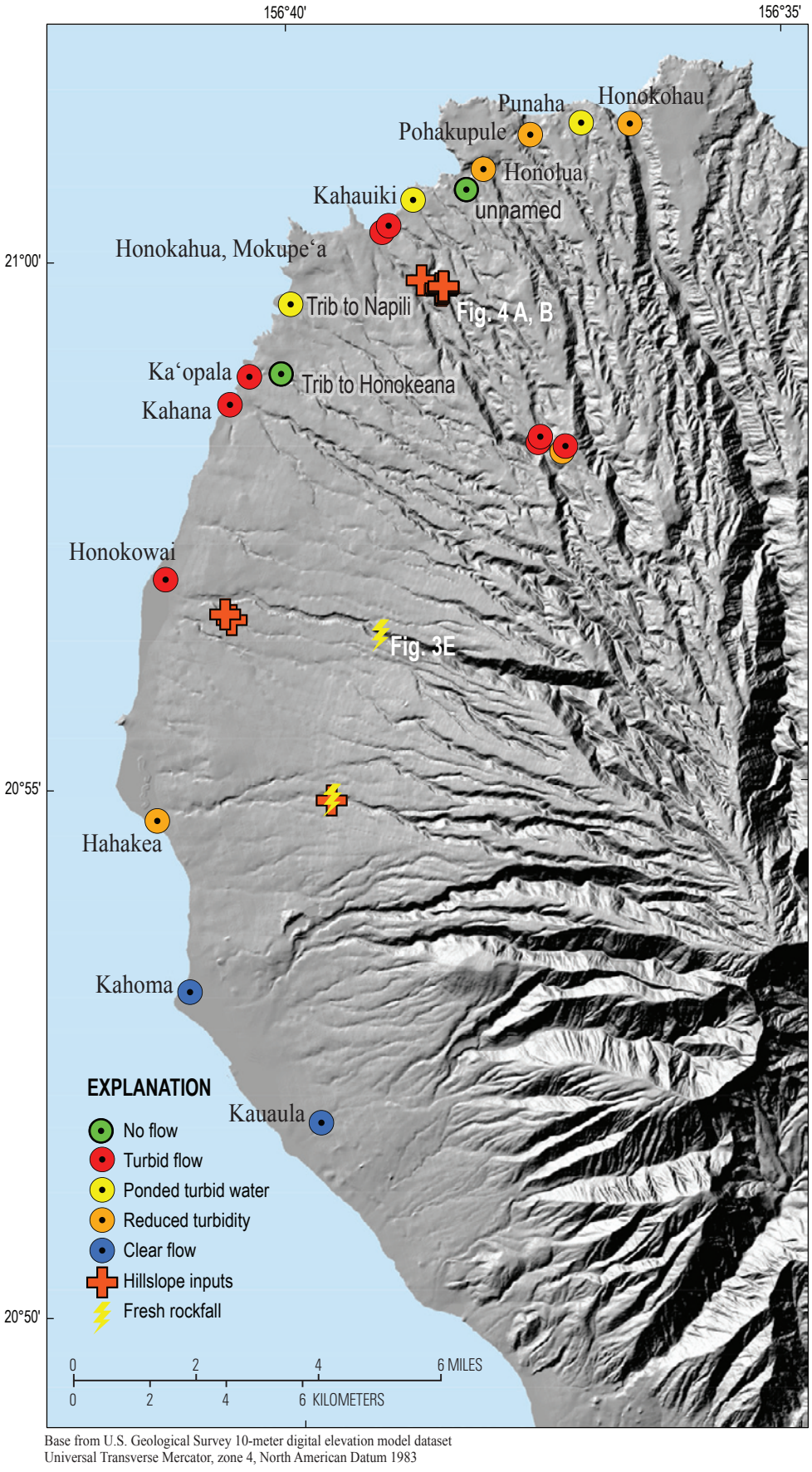

Base from U.S. Geological Survey 10-meter digital elevation model dataset
Universal Transverse Mercator, zone 4, North American Datum 1983

Figure 12. Map showing locations of stream-sediment pollution observed July 20, 2014, 13:00–18:00 HST, following the July 19–20 storm. The most turbid runoff occurred in streams between Honolua and Honokōwai. In these streams we observed orange- or red-orange-colored turbidity. Those with reduced turbidity had brown-colored suspended sediment. Rainfalls occurred from 06:00 to 08:00, 5–7 hours prior to the beginning of these observations. Hillslope inputs include fine sediment from overland flow and small gullies active during or after the storm, as observed on July 20, 2014. Fresh rockfalls may have been triggered by this storm. This historically small storm created sediment plumes at much of West Maui's northwest coast (see figs. 10, 11). Trib, tributary.

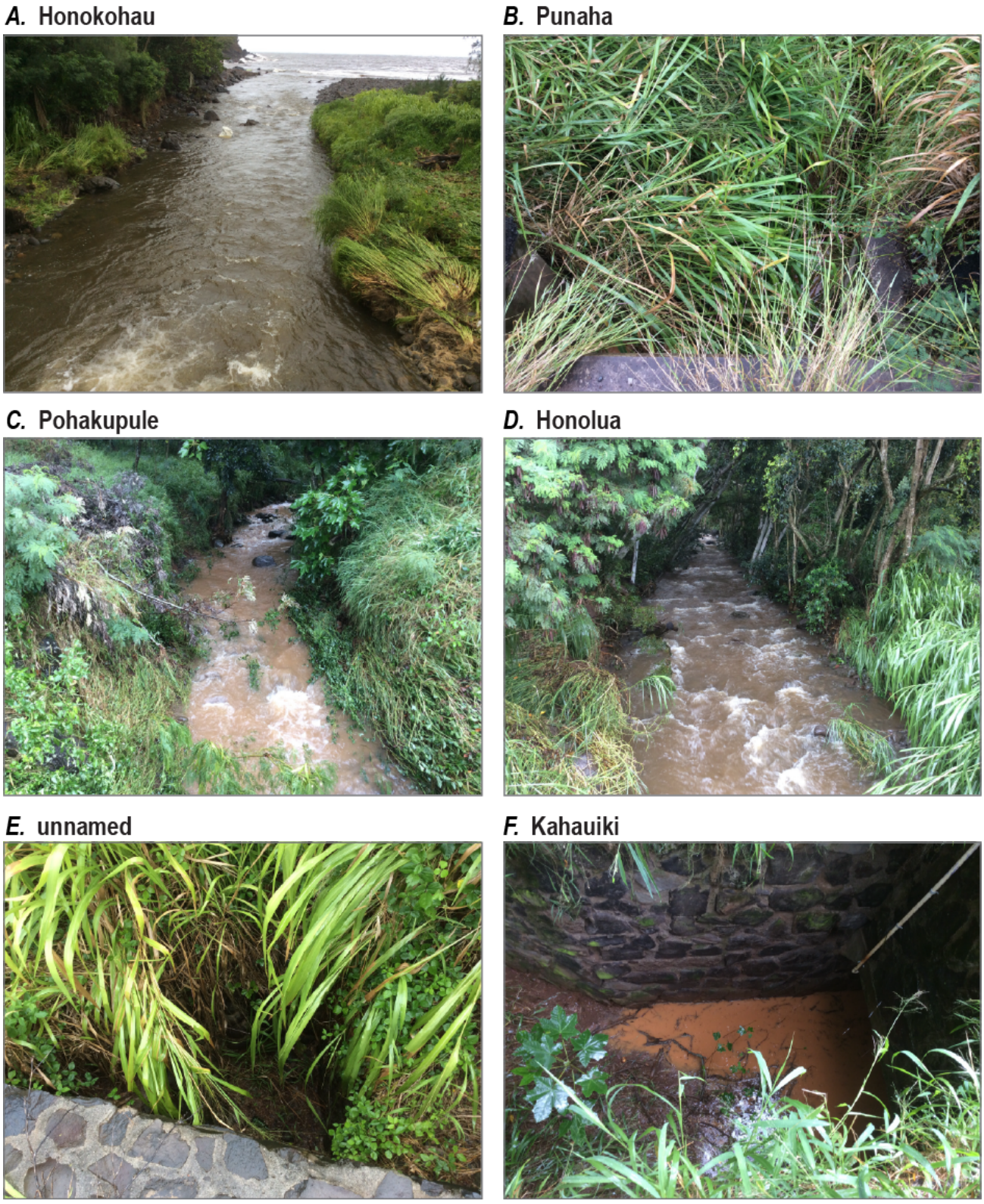

Figure 13. Photographs of suspended sediment in West Maui streams (from north to south), observed July 20, 2014, 13:00–18:00 HST. *A*, Honokōhau Stream. *B*, Pūnahā Gulch. *C*, Pōhakupule Gulch. *D*, Honolua Stream. *E*, Unnamed tributary to Honolua Bay near Honokohau Street. *F*, Kahauiki Gulch. *G*, Confluence of Honokahua Stream (right) and Mokupe‘a Gulch. *H*, Tributary gulch to Nāpili Bay. *I*, Tributary gulch to Honokeana Bay. *J*, Ka‘ōpala Gulch outlet. *K*, Kahana Stream. *L*, Honokōwai Stream; *M*, Hāhākea Gulch outlet ~10 m up from coast. *N*, Kahoma Stream from Front Street bridge in Lahaina. The highest sediment concentrations from this storm are in streams between Kahauiki Gulch (*F*) and Honokōwai Stream (*L*).

G. Mokupe'a (l), Honokahua (r)

H. Tributary to Napili

I. Tributary to Honokeana

J. Ka'opala

K. Kahana

L. Honokowai

M. Hahakea

N. Kahoma

Figure 13.—Continued

Infiltration Rates

Infiltration rates from fields and roads of West Maui (fig. 6, table 3) range from 12 to 93 mm/hr. This range is consistent with values found for agriculturally treated soils on O‘ahu, which are between 11 and 85 mm/hr if four outlying points are excluded (table 4 in Green and others, 1982). Disked pineapple fields in West Maui encompass this full range, although the majority of rates are greater than 25 mm/hr. The absence of widespread runoff from fields after rainfalls of July 19–20 (for example, fig. 7*B*) is consistent with the fact that rainfalls did not exceed these K_{sat} values. The absence of valley networks cut into these features over the last 1.1–1.3 Ma is also consistent with hydraulic conductivities that often exceed rainfall intensities. Unimproved dirt roads, both loose and compacted, range from 30 to 56 mm/hr. We noticed little runoff from these sources as well (fig. 7*A*). The air-fall deposits capping West Maui have a median grain size of fine sand, less than ~25 percent silt, and less than 5 percent clay (fig. 14). They are coarser than air-fall deposits from the island of Hawai‘i (red curve in fig. 14). Most soils in the former agricultural fields plot as loamy sands on the USDA soil classification chart (fig. 15).

Table 3. Matrix infiltration estimates of saturated hydraulic conductivity and corresponding recurrence intervals for rainfalls.

[Ksat, saturated hydraulic conductivity, mm, millimeters; mm/hr, millimeters per hour; USDA, U.S. Department of Agriculture]

Land use	K_{sat} (mm/hr)	1-hour recurrence (years)	2-hour recurrence (years)	Last 1-hour event	Last 2-hour event	Soil classification (USDA)	d50 (mm)	Sample	E	N
		Lahaina / Field 46		Field 28 / Puu Kolii					UTM NAD 83 Zone 4	
Disked pineapple field	93	>23.9 / 13.8	-	Mar 2012 / Jan 2011	Dec 2007 / Dec 2007	Silt loam	0.19	md13	741603	2314141
Compacted dirt road	82	>23.9 / 9.2	-	Mar 2012 / Jan 2011	Dec 2007 / Dec 2007	Silt loam	0.37	md7	746343	2316368
Disked pineapple field	72	>23.9 / 5.5	-	Dec 2011 / Dec 2007	Dec 2007 / Dec 2007	Silt loam	0.23	md1	741687	2313573
Disked pineapple field	66	>23.9 / 3.9	-	Mar 2012 / Jan 2011	Dec 2007 / Dec 2007	Silt loam	0.16	md3	742237	2313880
Disked pineapple field	63	>23.9 / 3.9	-	Mar 2012 / Jan 2011	Dec 2007 / Dec 2007	Silt loam	0.18	md2	741860	2313966
Compacted dirt road	56	23.9 / 2.5	-	Jul 2014* / Mar 2012	Dec 2008 / Jan 2011	Silt loam	-	md8	746343	2316368
Loose dirt road	56	23.9 / 2.5	-	Jan 2011 / pre-2002	pre-2006 / pre-2002	Silt loam	0.34	md5	747149	2315987
Cane field	54	23.9 / 2.3	-	Mar 2012 / Jan 2011	Dec 2007 / Dec 2009	Silt loam	0.21	md4	742801	2314070
Disked pineapple field	39	6.0 / 0.81	- / 27.6	Jan 2011 / Dec 2007	Dec 2007 / pre-2002	Silt loam	0.19	md11	741603	2314141
Compacted dirt road	33	4.0 / 0.47	- / 5.5	Jul 2014* / Mar 2012	Dec 2008 / Jan 2011	Silt loam	-	md6	747149	2315987
Disked pineapple field	32	4.0 / 0.47	23.9 / 5.5	Dec 2011 / Dec 2007	Dec 2007 / Nov 2006	Silt loam	0.19	md12	741603	2314141
Disked pineapple field	26	1.8 / 0.32	12 / 3.1	Jul 2014* / Mar 2012	Dec 2008 / Jan 2011	Silt loam	0.16	md10	741278	2314110
Disked pineapple field	12	0.29 / 0.06	0.83 / 0.61	Jul 2014* / Mar 2013	Jul 2014 / Jan 2013	Silt loam	0.13	md9	741259	2314100

*Rainfall data from Honokowai-lower tipping bucket gage.

Table 4. Reconnaissance sediment budgets.

[Soil bulk density of 950 kg/m^3. m, meters; m^2, square meters, mm/a millimeters per year; italics indicate values from scenarios]

Process	Area/length ((m^2)/m)	Percent of area	Modeled lowering rate (mm/a)	Modeled suspended load (metric tons/yr)
Honolua watershed				
Whole catchment	10,967,300	100	0.03	313
Rockfall	3,958,353	36	0.03	113
Soil creep—canopy	5,689,001	52	0.03	162
Soil creep—no canopy	367,850	3	0.03	10
Overland flow—lumped	-	-	-	-
Agricultural fields	11,707	-	0.10	1
Agricultural fields	11,707	-	1.00	11
Hotspots	-	-	-	-
Valley deposits—undivided	686,037	6	0.00	0
high bank erosion, 50% length exposure	*14,612*	-	100.00	1,388
medium bank erosion, 50% length exposure	*14,612*	-	10.00	139
low bank erosion, 50% exposure	*14,612*	-	1.00	12
high bank erosion, 10% length exposure	*2,922*	-	100.00	250
medium bank erosion, 10% length exposure	*2,922*	-	10.00	25
low bank erosion, 10% length exposure	*2,922*	-	1.00	2
Terrace	251,797	2	0.00	0
Honokōwai watershed				
Whole catchment	10,615,700	100	0.03	414
Rockfall	4,943,364	47	0.03	174
Soil creep—canopy	2,850,623	27	0.03	100
Overland flow—lumped	-	-	-	-
Agricultural fields	1,938,334	18	0.10	227
Agricultural fields	1,938,334	18	1.00	2,268
Hotspots	-	-	-	-
Valley deposits—undivided	632,531	6	0.00	0
high bank erosion, 50% length exposure	*14,253*	-	100.00	1,668
medium bank erosion, 50% length exposure	*14,253*	-	10.00	167
low bank erosion, 50% exposure	*14,253*	-	1.00	17
high bank erosion, 10% length exposure	*2,851*	-	100.00	334
medium bank erosion, 10% length exposure	*2,851*	-	10.00	33
low bank erosion, 10% length exposure	*2,851*	-	1.00	3
Terrace	217,618	2	0.00	0
Talus	33,230	0	0.00	0

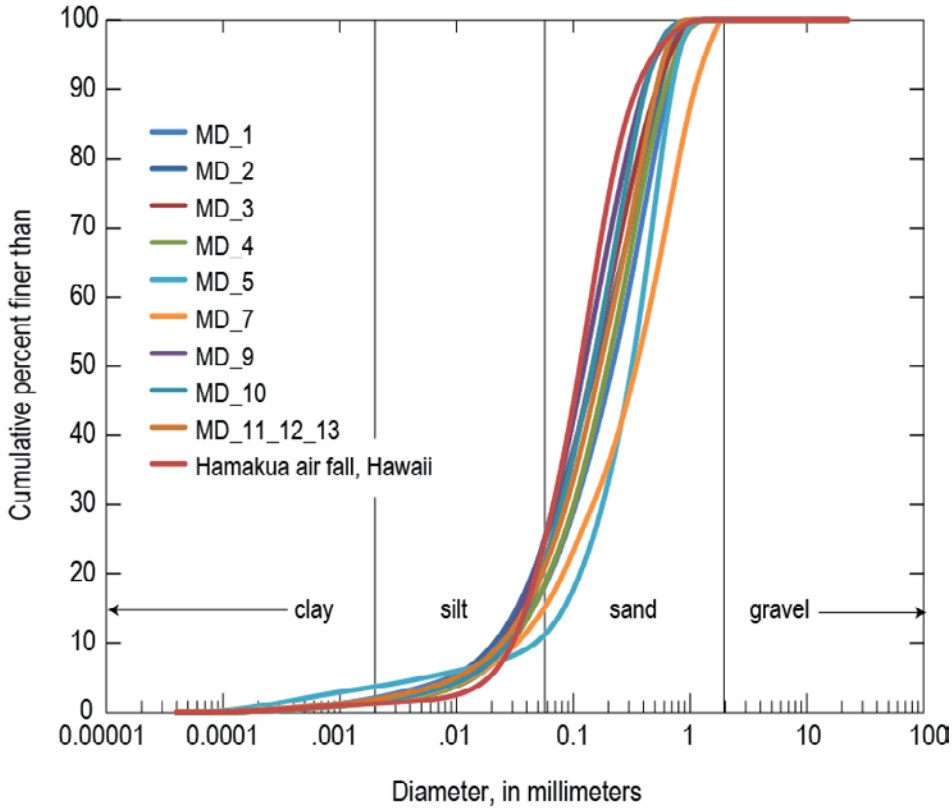

Figure 14. Plot of particle-size distributions of surface soils from infiltration test sites on fields and roads of West Maui (see figure 6 for locations, table 3 for results). These air-fall deposits capping West Maui have a median grain size of fine sand, are less than ~25 percent silt, and less than 5 percent clay. They are coarse compared to similar air-fall deposits from Hawai‘i Island.

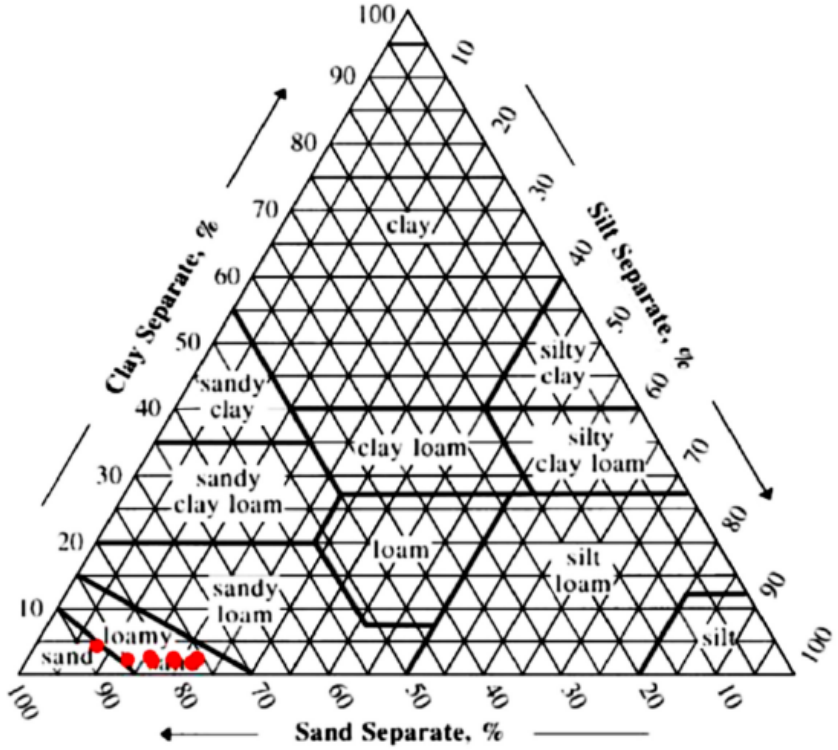

Figure 15. Diagram of particle-size distributions from figure 14 (red dots) plotted on the USDA soil classification diagram. Many of the samples are so close in grain-size distribution that they overlap on this plot. The air-fall deposits capping this part of West Maui are loamy sands. % is percent.

Rainfall Analysis

Rain gages from the uplands of West Maui show that over the past three decades (1) annual rainfall totals have gone down (fig. 16), (2) cumulative hours of rainfall at intensities greater than 20 mm/hr have also gone down (fig. 17), but (3) the frequency of storms with continuous intense rainfall has not (fig. 18). In short, although total rainfall has decreased, more rainfall now occurs during intense storms capable of causing runoff and erosion. As an example, the December 5, 2007 storm is the most intense storm during the ~30-year record at these gages, with rain sustained for ~2 hours at rates greater than 40 mm/hr (table A7).

Annual rainfall totals have decreased during the period of record at three West Maui gages. Although there is great annual variability, Field 46 totals declined from about 1,500–3,500 mm in the 1980s, to values of 1,000–2,000 mm in later decades. Field 28 and Puu Kolii continue this downward trend. The amount of intense rain each year also shows a downward trend (fig. 17) for these three gages; hours of intense rainfall decreased by about three to five times over the last 27 years at Field 46, depending on which threshold value is used. Downward trends are weaker at Field 28 and Puu Kolii. At these gages, rainfalls exceeding 50 mm/hr, which would trigger runoff on many unimproved roads and former agricultural fields, have occurred for minutes to a few hours annually over the last decade. By contrast, there are no apparent trends for coastal Lahaina rainfalls over the last three decades (figs. 16, 17A). Rainfalls in excess of 50 mm/hr are uncommon, occurring only during a period of a few years on either side of 1990.

Figure 18 (and tables A5–A8) show events when it rained for more than 1 hour at rates above 20 mm/hr. We chose this value because more than 90 percent of the K_{sat} values in table 3 exceed it. These events represent the storms most likely to generate erosion and runoff. The Lahaina and Field 46 gages recorded about one of these events per year during the 1980s (tables A5, A8), and less than that during the 1990s. Lahaina had only two during the 1990s, whereas Field 46 had just below one per year on average. So the occurrence of these greater than 20 mm/hr events is reduced in the period from 1993 to 2001. In the 2000s, Puu Kolii and Field 28 both had about one event per year. The very largest storms, with continuous rainfall greater than 40 mm/hr, would activate runoff at a number of the former agricultural field sites in table 3. These largest storms did not occur between 1978 and 1988 or 2007 and 2014.

Rainfalls from individual storms are compared in figure 19, which illustrates historic storms at Field 46 and Puu Kolii. As rainfall intensity increases, there is an exponential decline in the number of hours with rainfall greater than that intensity. Most storms have an intercept of ~4, and slope values of ~0.05. The similarity of the curves at this scale suggests that these storms came from a similar population. The storm of May 5, 1987 was exceptional for its long-duration and high-intensity rainfall. The storm of December 5, 2007 is the most intense storm of record, with a rainfall intensity greater than 40 mm/hr lasting for more than one hour.

Another way of collapsing the rainfall data is to compare the recurrence intervals for 1-hour and 2-hour rainfall intensities. Figure 20 illustrates the average return interval for a given rainfall intensity. For similar recurrence intervals, it rains twice as much in the north (Field 46) as it does in the south (Lahaina). This difference diminishes for 2-hour intensities. Our sample locations at sandy agricultural fields would therefore experience brief runoff from greater than 50 mm/hr rainfall intensities about once a decade near Lahaina, but every 1.5 years at Field 46. Sustained runoff from agricultural fields for more than 1 hour would be very rare because intensities greater than 50 mm/hr sustained for 2 hours are not present in the over 2-decade-long records. Because rainfall totals have decreased through time, these recurrence intervals may now be larger. Disking marks remain in the fields from the last agricultural treatment around 2012, indicating that storms of this intensity have not occurred since then.

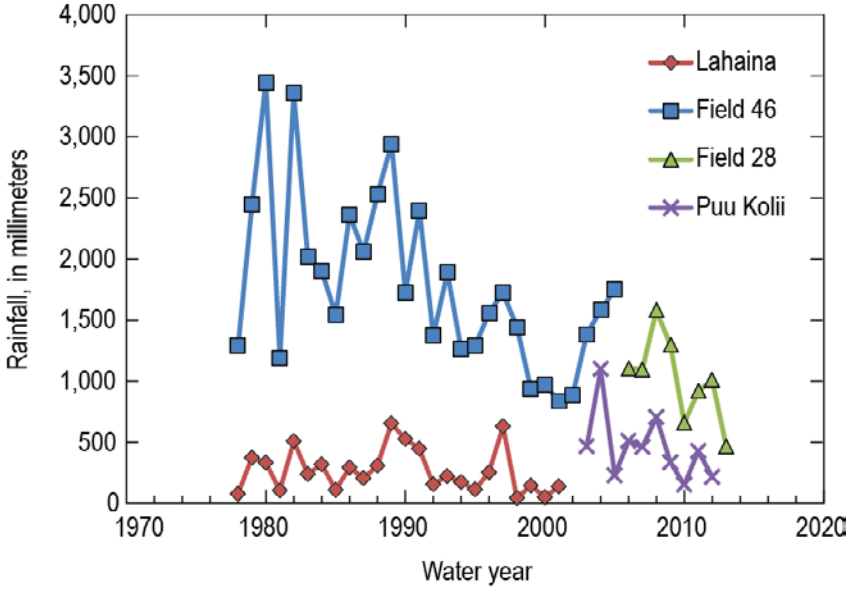

Figure 16. Plot of historic rainfall data from West Maui rainfall gages (locations in figure 6). A water year starts on October 1. Although there is great annual variability, the trend shows rainfall has decreased over the last three decades at the central and northwest gages. There is no evident trend at the arid south-central coastal gage at Lahaina. The decline in the north is perhaps a consequence of reduced trade-wind-driven rainfalls.

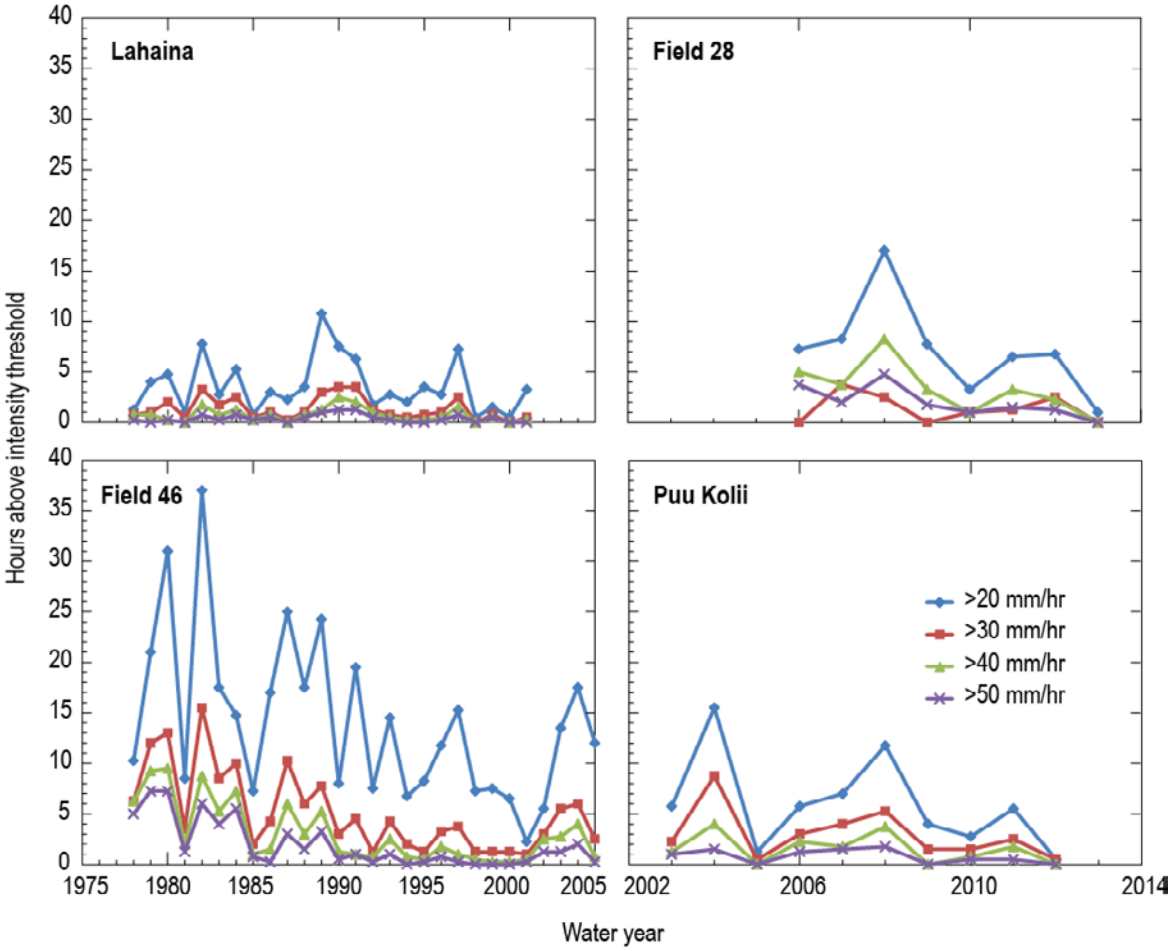

Figure 17. Plots of historic rainfall intensity data from West Maui rainfall gages (locations in figure 6). See appendix for historic storm records corresponding to these graphs. Lahaina gage record is similar to rainfall totals, rainfall intensity data show no systematic trend over the record. Heavy rainfalls (>20 mm/hr [millimeters per hour]) have occurred 1–11 hours per water year over this record. Field 46 gage record shows a decrease in the frequency of the heaviest rainfalls from 1978 to 1992, with no evident pattern after that year. After 1992, there were about 3–17 hours per water year of heavy rainfalls (>20 mm/hr). Nearby Field 28 gage record shows 1–17 hours of heavy rainfalls per water year. Totals after 2008 are somewhat lower than previously. Puu Kolii gage record illustrates a similar reduction in the frequency of heavy rainfalls since 2008.

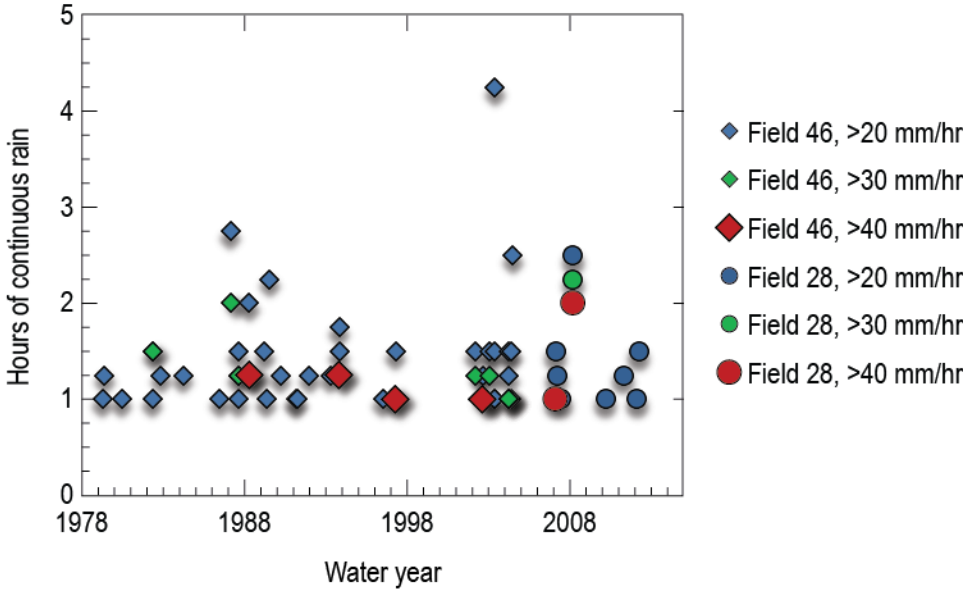

Figure 18. Plot showing occurrence of largest storms in West Maui uplands since 1978. See tables A7, A8 for source data. Symbols represent hours (>1) of rainfall at rates greater than 20, 30, and 40 mm/hr (millimeters per hour). The occurrence of these most intense, continuous rainfalls has not varied systematically over this period, even as the total hours of intense rainfall and annual rainfall totals have declined. These storms may represent the population of rainfall events most likely to result in steepland erosion and runoff.

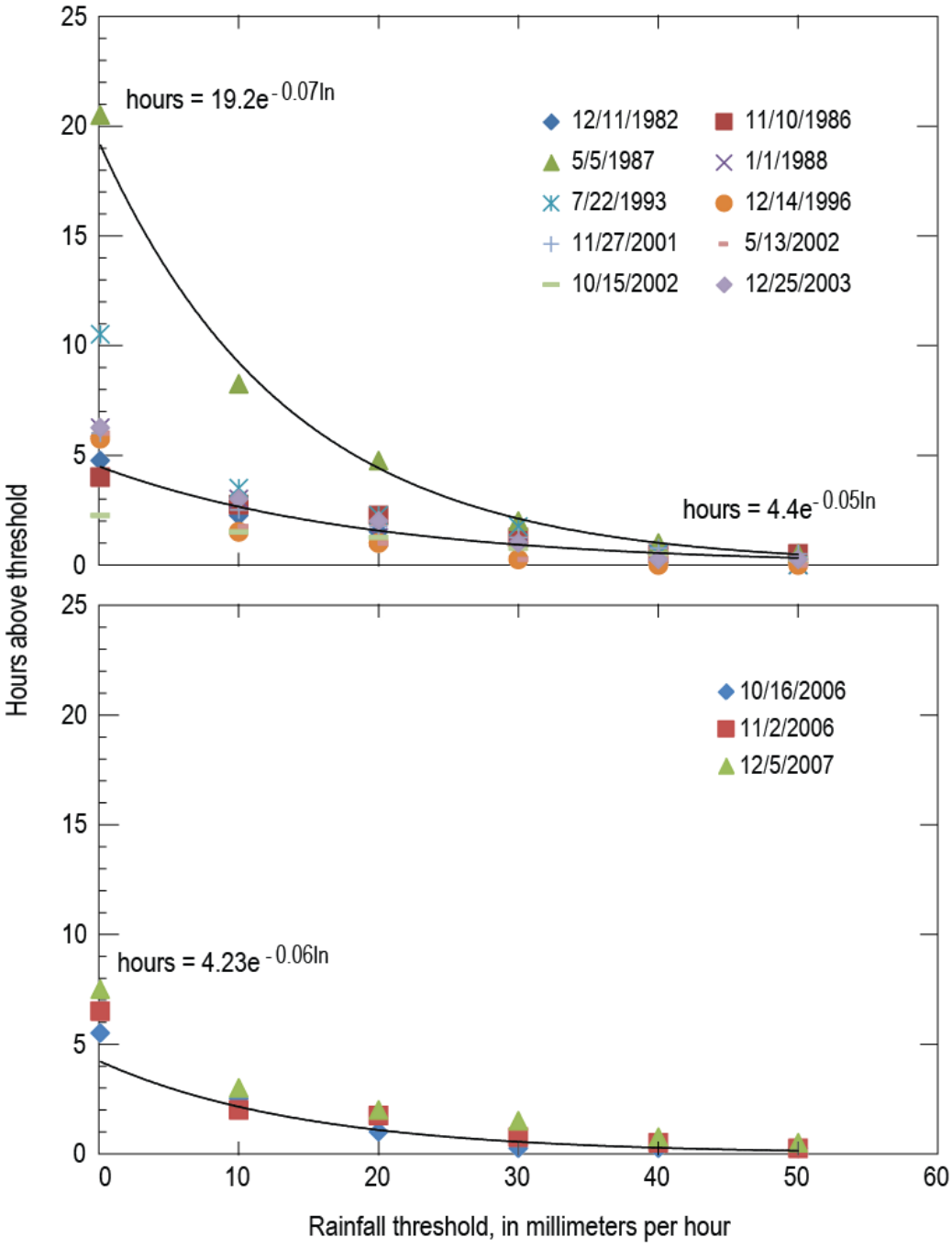

Figure 19. Plots showing cumulative exceedance rainfall intensities for the largest storms over the record of Field 46 (top) and Puu Kolii (bottom). Storm of May 1987 was one of the longest storms on record, although not the most intense, with over 5 hours of rainfall at intensities greater than 20 millimeters per hour. The intensity structure of the remaining storms at Field 46 and Puu Kolii appear similar, as evidenced by nearly equal intercept (4.2, 4.4) and similar slopes (-0.05 to -0.06). These smaller storms appear to be the characteristic heavy rainfall event for West Maui, and are the biggest historic events found in tables A5–A8.

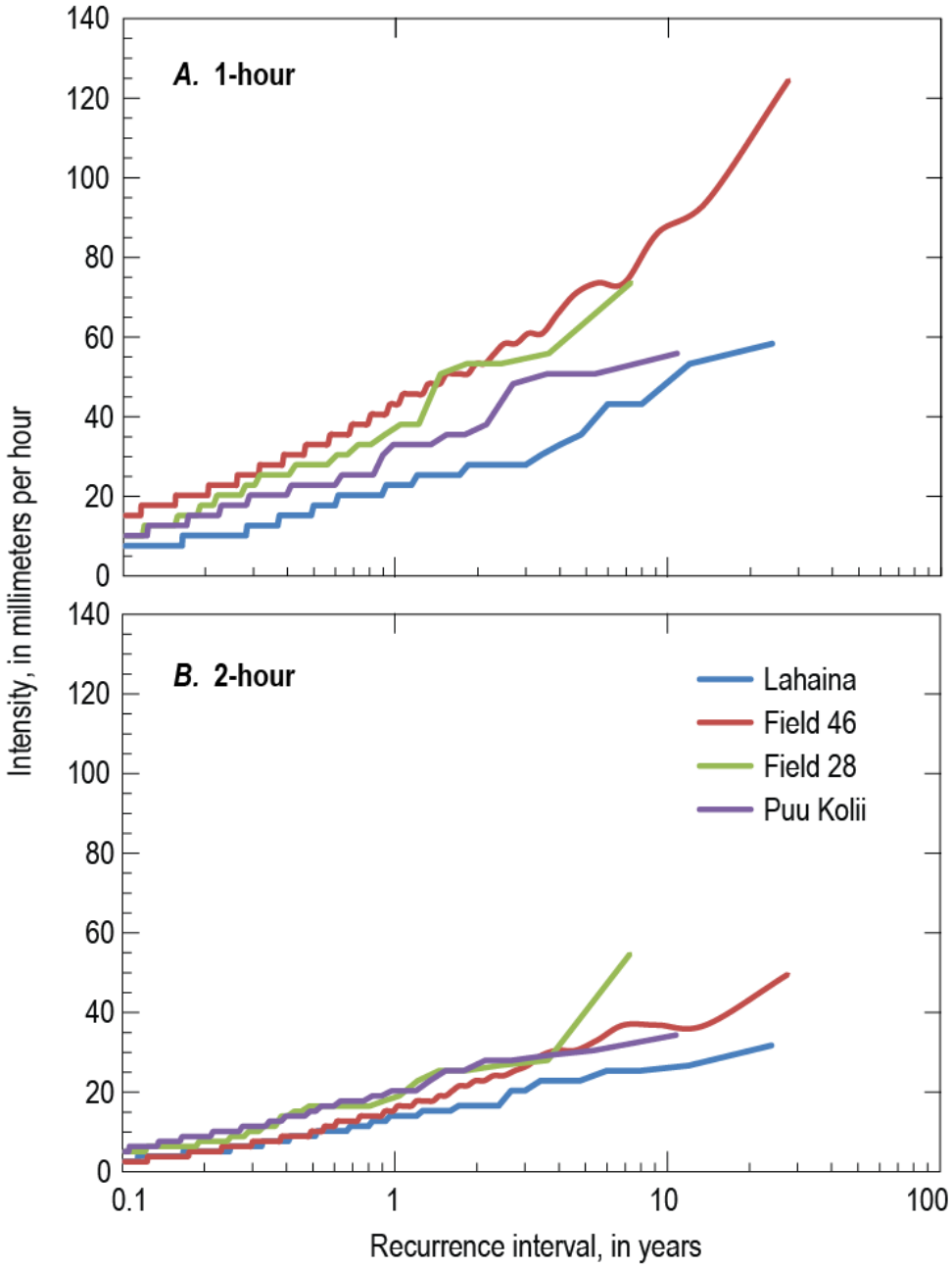

Figure 20. Plots of recurrence intervals for 1-hour rainfall intensities (A) and 2-hour rainfall intensities (B) in West Maui. See figure 6 and table 2 for locations and values, respectively, and text for details and limitations of records. Rainfall intensity for a given recurrence interval is roughly twice as high in the north (Field 46) as it is in south (Lahaina). This difference diminishes for 2-hour intensities. Many of the sandy agricultural fields would experience runoff from greater than 50 millimeters per hour rainfalls only about once a decade in the Lahaina area, and every 1.5 years at Field 46. Because rainfall intensities have decreased through time, the current recurrence intervals could be much longer, as evidenced by the disking marks that remain in the fields from the last treatment over 3 years ago. Runoff from agricultural fields for over 1 hour would be very rare because 2-hour intensities greater than 50 millimeters per hour are not present in the over 2-decade-long records.

Geomorphic Process Map

Figure 21 illustrates one view of the distribution of geomorphic processes in Honolua and Honokōwai watersheds. Uplands are characterized by rockfall (for example, fig. 3*D*) and soil creep (for example, fig. 3*A*, *B*), occurring in forested areas with largely intact canopy. Processes that create coarse sediment, such as rockfalls and landslides, occupy large amounts of Honolua (36 percent) and Honokōwai (47 percent) watershed areas. Lava flow edges crop out as continuous bands along many steep valley walls (fig. 3*D*), illustrating the lack of soil. Flutes as wide as 10 to 100 m cut some valley walls (fig. 3*D*), consistent with episodic scour by debris flows and rockfall. A few talus deposits are sufficiently large to appear in both DigitalGlobe imagery and 10-m topography; most are too small to map. Large (>100-m-wide) bedrock landslides cut into low-relief surfaces of both watersheds. In Honolua and Honokahua, the landslides are concentrated upstream of lineaments that may be the surface expression of dikes. Large (>3 m relief) debris flow and fluvial terraces downstream of the landslides are consistent with an episodic release of coarse sediment that aggraded the valley bed, followed by incision. In the headwaters of Honokōwai, we observed similar terraces composed of unsorted sediment lacking imbrication, consistent with deposition by debris flows (for example, fig 5*B*). Along with smaller fluvial, debris flow, and historic terraces, gravel and coarser grains arranged in pool-riffle, plane-bed, step-pool, or cascade bedforms (fig. 5*A*, *C*) make up the valley deposits unit.

Soil creep in low-relief, canopied areas occupies large fractions of Honolua (52 percent) and Honokōwai (27 percent) watersheds. Soil creep in grasslands (for example, golf courses) occupies a small portion of lower Honolua. Former agricultural fields (fig. 7*B*) are subject to Horton overland flow and occupy a large portion of Honokōwai (~20 percent). The current vegetation varies from full shrub cover to exposed soil.

A few isolated deposits from human land use, such as sidecast (fig. 4*E*), are shown in figure 21. These are found at the margins of former agricultural fields. A number of coalesced, shallow landslides occurred in the lower Honolua watershed (fig. 4*E*), but are not readily visible at the scale of figure 21. White lines on figure 21 show the maximum extent (~28 km) of potential bank erosion into historic terraces.

Reconnaissance Sediment Budget for Honokōwai and Honolua Watersheds

Table 4 lists modeled watershed annual suspended-sediment loads in the right-most column. In the first row, a low whole-catchment lowering rate (0.03 mm/a) applied to Honolua and Honokōwai watersheds produces suspended-sediment loads of 300–400 metric tons per year. Following rows list suspended loads by geomorphic process, starting with rockfall and soil creep rates. Each modeled load is the product of the mapped area of a geomorphic process and its fine-sediment production rate.

Rockfall and soil creep processes occur in large areas of both watersheds (74–91 percent), but sediment loads from these sources are ~200–400 metric tons per year because we assume slow lowering rates of 0.03 mm/a. Potential overland flow erosion rates of 0.1–1.0 mm/a produce low loads in Honolua, but potentially very large loads in Honokōwai (227–2,268 metric tons per year). Honolua has less agricultural field area that could generate overland flow (<1 percent) than Honokōwai (18 percent). We have no logic to assign lowering rates to these disturbed areas, beyond the values of ~2 mm/a measured at Moloka‘i for Horton overland flow erosion in partially vegetated soils. The lack of recent rills and gullies and high measured K_{sat} values are observations that suggest this source does not commonly erode.

The exposure and erosion rates of fine-grained historic valley terraces are not known. This source of uncertainty matters to sediment load estimates. If 50 percent of valley lengths have fine-grained historic terraces eroding at 100 mm/a, the resultant suspended load from this source is 1,400–1,700 metric tons per year. If only 10 percent of valley lengths have fine-grained historic terraces eroding at 1 mm/a, suspended-sediment loads are only 2–3 metric tons per year. Under certain combinations of exposure and erosion rate, bank erosion of historic terraces can dominate the suspended-sediment load from both watersheds.

Discussion

West Maui storms bring coastal sediment plumes that are plausibly sourced from erosion of historic terraces, a legacy of agriculture. These deposits were visibly eroded after the July 19–20, 2014 storm and were available at streamside for export to coastal plumes in the hours following highest rainfall intensities. Post-storm observations of historic terraces indicated that streams entrained sands, silts, and clays during bank erosion at high flow, and perhaps from in-stream sources under surface gravels. These deposits must have originated during historic times because of the artifacts that they contain (for example, drip-line fragments). 1950s-era aerial photographs show that valley sidewalls are locally covered by rilled aprons of sediment. One interpretation of this imagery is that bulldozers pushed mixtures of fine-grained sediment and boulders over planeze margins. The resulting aprons of material, eroded by overland flow in small alluvial fans, impinge on streamsides as historic terraces.

Other sources for plume sediment are less plausible. The storm brought rainfalls that were insufficient to generate overland flow in most of the former agricultural fields or unimproved roads of West Maui. The conductivity of these fine-grained deposits may control which rainfalls cause plumes. Field observations of disking marks and the absence of widespread evidence for overland flow (for example, rills and gullies) are consistent with the fact that measured infiltration rates exceed common rainfall intensities.

Runoff generation from former agricultural fields and unimproved roads seems to be occurring less often in the past decade. Rainfall in figures 16 and 17 declines in both annual

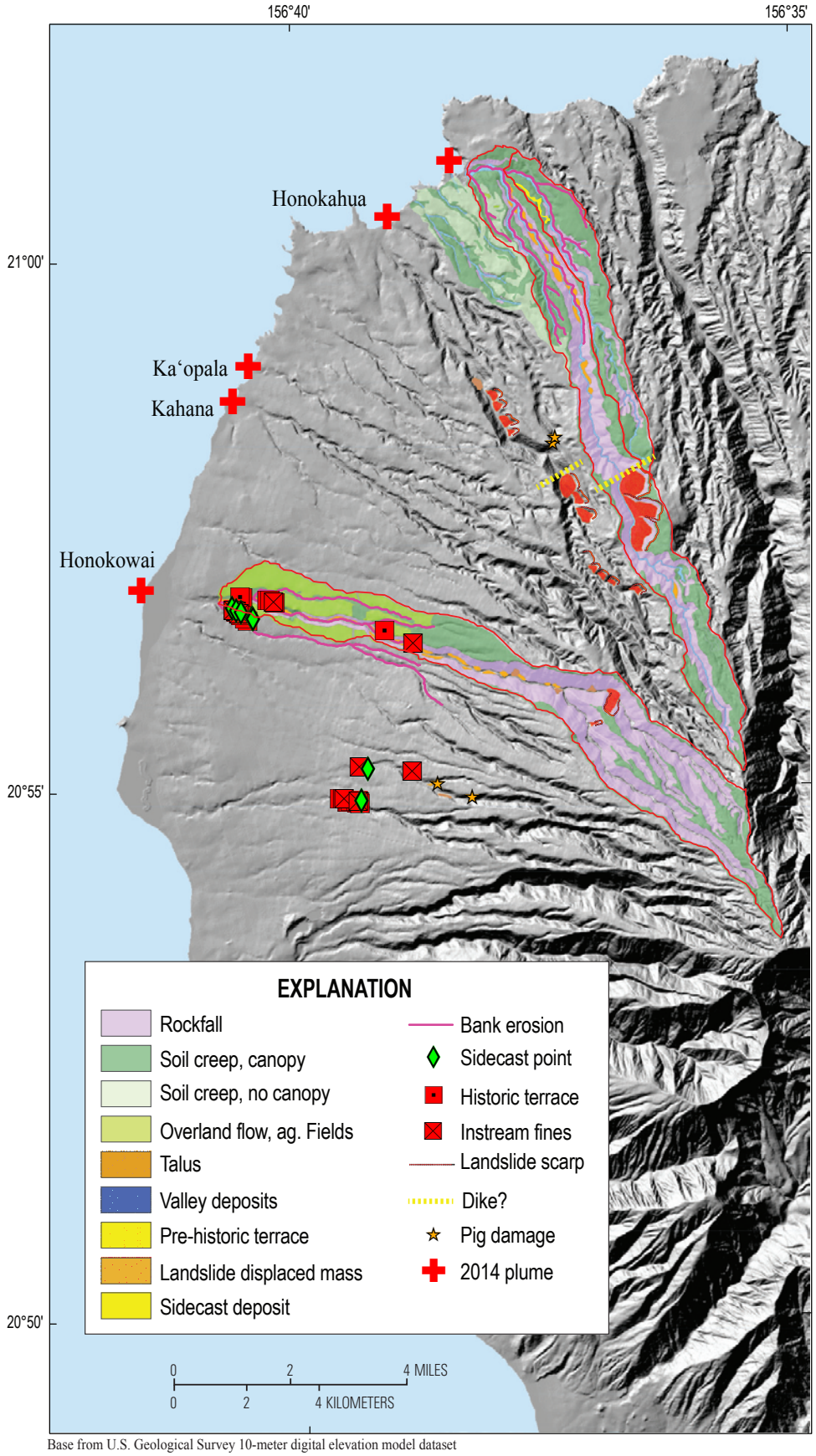

Base from U.S. Geological Survey 10-meter digital elevation model dataset
Universal Transverse Mercator, zone 4, North American Datum 1983

Figure 21. Reconnaissance geomorphic process map for two watersheds in West Maui (Honolua and Honokōwai). The map represents the predominant process that moves sediment in a given area, as determined by topography, DigitalGlobe imagery, and field reconnaissance. If each process can be characterized with a lowering rate, or range of lowering rates, the summation of these products can be used to estimate the sediment budget arriving at coastal areas. Both Honolua and Honokōwai have extensive areas where the predominant processes are rockfall or soil creep, which likely have very low rates of fine sediment production (<<0.1 millimters per year). Both may have extensive (~14 km) reaches of potential bank erosion. ag., agricultural.

total and cumulative hours greater than a given intensity. This is consistent with regional studies (see, for example, Chen and Chu, 2014; Timm and others, 2013) showing a decline in the occurrence of "heavy" rainfall. Timm and others (2013) defined heavy rainfall as days whose rainfall totals exceed the 90th percentile of recorded rainy days. Like the declining trend in annual rainfall totals of figure 16, they found a decrease in the occurrence of heavy rainfall days in Hawai'i since the mid-1970s, and their models show that there will likely be fewer of these heavy rainfall days in the future.

This definition of heavy rainfall, however, does not indicate rainfall rates that cause erosion and runoff. These values must be defined by rainfall intensities that exceed geomorphic thresholds (for example, K_{sat} values) and initiate processes such as Horton overland flow, or the generation of positive pore pressures causing landslides. Figure 18 shows no temporal trend for these geomorphically important storms. Illustrating this, the storm of record at Field 28 gage occurred in December 2007 (the highest red circle in fig. 18). On Moloka'i, the same storm led to as much as 1.6 cm of soil lowering (Stock and others, 2009, 2010), the largest amount observed to date (2006–2015). Its effect on West Maui may have been similarly large. Consequently, one view is that although lower intensity rainfalls have declined in frequency, changing and possibly reducing vegetation cover, the occurrence of geomorphically effective rainstorms has not detectably changed. This combination increases susceptibility to erosion, producing greater suspended-sediment loads. The future may bring less vegetation cover, and consequently more erosion from the same intense storm population.

Erosion rates in the reconnaissance sediment budget have great uncertainties. For instance, the bank erosion part of the sediment budget depends on bank erosion rate and exposure, and on assumptions of fine sediment production from large areas of soil creep and rockfall. In the Methods section, we reasoned that suspended loads from rockfall areas and from heavily vegetated soil-creep areas would be below 0.1 mm/a. As a crude test of the notion that this value approximates the suspended load from rockfall areas, we plotted lowering rates calculated from suspended-sediment yields on O'ahu, Moloka'i, and Kaua'i (fig. 22). These values, expressed as the point lowering rate of a 950-kg/m^3-density soil, range from 0.03 to 0.8 mm/a for records over 5 years in length. The majority of measurements are biased towards areas where disturbance has created a water-quality problem requiring monitoring. These include loss of vegetation (see, for example, Stock and Tribble, 2010), construction (for example, north Hālawa Valley, O'ahu), and in-channel modifications (for example, Waikele on O'ahu). These sediment yields are much greater than 0.1 mm/a. Moanalua, O'ahu, the only watershed with relatively intact vegetation and a lack of disturbance, has a sediment yield equivalent to a soil lowering rate of 0.05 mm/a. This watershed is the least-disturbed watershed and has a steepland headwater with intact canopy. It is perhaps the most comparable to the rockfall and soil creep portions of Honokōwai and Honolua on Maui. This value is crudely consistent with the value of 0.03 mm/a suspended load production we assume for soil creep and rockfall areas of West Maui.

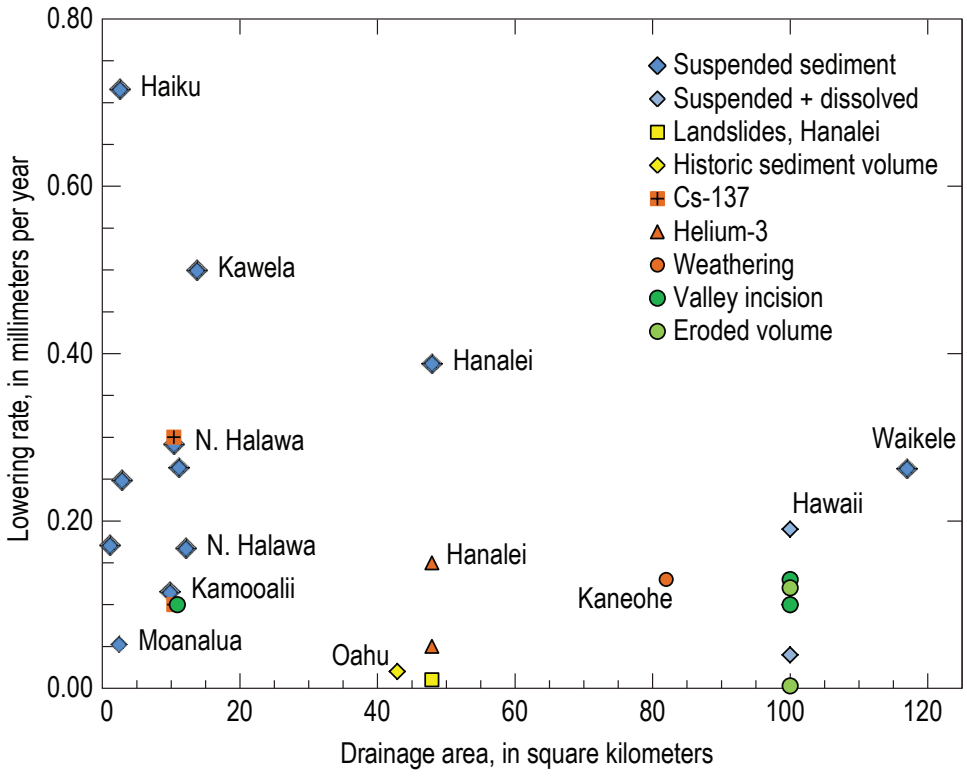

Figure 22. Published erosion rates for the islands of Kaua'i, O'ahu, Moloka'i, Lāna'i, and Hawai'i, expressed as a 950 kg/m^3 bulk-density soil-lowering rate. See table 5 for source data. Rates from suspended-sediment yield exclude bedload, which may be substantial (>10 percent by weight). Rates from valley incision omit hillslope processes, which may also be substantial. Terrain that is altered by vegetation loss or construction (for example, Ha'ikū, Kawela, and Hālawa) have lowering rates in excess of 0.2 millimeters per year. Long-term valley incision rates are approximately 0.1 millimeters per year. The least disturbed landscapes have lowering rates from 0.01 to 0.05 millimeters per year (for example, Moanalua, NF Kaukonahua). These rates may approximate the yields from undisturbed terrain dominated by soil creep and rockfall.

Lowering rates generated by rainsplash and Horton overland flow in former agricultural fields are unknown. A case can be made that many of these areas experience sustained (>1 hour) runoff less than once a decade (for example, fig. 20*A*, Field 46). Corresponding lowering rates must be small over the last million years, given the absence of channelization into these planeze surfaces. This lack of channelization makes it unclear how effectively field areas are hydrologically connected to main stem valleys. Decades of field engineering may have isolated runoff in many, though certainly not all fields. This is important because fewer fields almost certainly experience runoff from sustained periods of greater than 30-mm/hr rainfall. For instance, areas with K_{sat}<30 mm/a in table 3 could experience brief periods of runoff and erosion every half-year at Field 46 (fig. 20). Whether or not such areas contribute to coastal plumes depends on connectivity to the valley network.

Large landslides mapped in figure 21 are covered by canopied forests with no contrast at landslide boundaries. We interpret them to be prehistoric. Downstream of the slide body, some valleys widen abruptly. This boundary sometimes coincides with lineaments normal to the valley axis, which are possibly the surface expression of dikes (fig. 21). One hypothesis is that elevated-water tables upstream of dikes that cut across the valley slopes increase the susceptibility to deep-seated failures. The resultant large landslides act to widen the valley above the dikes, and produce large volumes of coarse material that migrate downstream, aggrading the valley. Following incision, these deposits remain as the many paired terraces on figure 21. If this is a common sequence of events, many Hawaiian valleys owe their width and sidewall profile to large landslides. Consequently, the majority of the erosion of Hawaiian edifices may be accomplished by large landslides, with boundary lowering driven by debris flow incision of valleys. The widespread presence of debris flow deposits above 3–5 percent valley gradients on Moloka‘i and West Maui would be consistent with this hypothesis.

Measurements Needed for a More Authoritative Sediment Budget

The reconnaissance sediment budget has great uncertainties that could be reduced by a few key field observations and monitoring. The extent and erosion rate of historic terraces is not known. Notional calculations (table 4) show that, for erosion rates similar to those measured in Moloka‘i, bank erosion of these deposits dominates suspended loads. Field observations could delineate depth and extent of historic terraces and the fraction of their length exposed to erosion. A similar effort could be made to estimate the length of the stream network where pig activity is supplying fine sediment to the streams. Estimates of erosion rates from both processes are needed, so that we can assess the mass of these contributions to suspended sediment.

Estimates of suspended-sediment concentration or turbidity lower in the valley network could also be used to test hypotheses for the source of fine sediments. If erosion of historic terraces in lower reaches is the predominant source of pollution, sediment concentrations should increase dramatically along these reaches. It would be useful to test the hypothesis that turbidity color (red orange versus brown in fig. 12) is indicative of sediment source. Red-orange-colored turbidity might be a proxy for erosion of historic terraces.

There is a need to understand what sustained, heavy rainfalls (for example, December 2007) would do to the former agricultural fields. If drainage is sufficiently isolated from the main valleys, runoff will not contribute to plume generation. If not, the loading could be substantial, if infrequent. High-resolution topography from lidar or imagery is needed for this task.

Conclusion

A case can be made that sediment plumes of West Maui are largely sourced from bank erosion of historic terraces. Field observations during and after the July 2014 storm indicate that other sources either are not connected or are not contributing runoff for storms of this intensity. Measured hydraulic conductivities of fields and roads mostly exceeded the rainfall intensities from this storm. So, treatments of former agricultural fields, roads, and reserve forests are not likely to measurably affect sediment pollution from smaller, more frequent storms. Comparison of rainfall records to measured infiltration rates indicates that only parts of former agricultural fields are capable of generating runoff during historic storms. Storms with rainfall intensities capable of eroding agricultural fields for an hour or longer occurred four to five times per decade during the 1980s and 2000s and only twice during the 1990s. Although annual rainfall totals have decreased over the last three decades, there is no evidence that geomorphically effective storms have become less frequent. Consequently, storms of the future may have more impact on a landscape with lower moisture availability.

A reconnaissance sediment budget indicates that bank erosion rates and length of exposure of historic fine-grained terraces are major uncertainties in estimating the sources of fine sediment loading to the coastal waters of West Maui. The presence of coastal plumes from some streams does indicate that upstream sediment-retention basins are not stopping the load from all small storms. If development proceeds, experience in urbanized systems indicates that high flows will become more frequent as concrete and asphalt surfaces concentrate rainfall from more rapid runoff into stream channels. Higher, more frequent flows will accelerate bank erosion without a countervailing influence. In short, continued development of West Maui has the potential to exacerbate sediment plumes unless there is an effective strategy to reduce bank erosion.

Table 5. Literature estimates of Hawaiian lowering rates.

[For island-wide analyses, we used a default area of 100 km^2. Abbreviation: PIWSC, Pacific Islands Water Science Center, USGS]

Area (km^2)	Minimum (mm/a)	Maximum (mm/a)	Period of averaging (years)	Method	Location	Reference
100	0.003	0.12	$1.5–4.4\times10^6$	Eroded volume	Kauaʻi	Ferrier and others, 2013
100	0.13	-	$3.5–4.0\times10^6$	Valley depth	Waimea, Kauaʻi	Li, 1988
100	0.1	-	$1.8–3.0\times10^6$	Valley depth	Oʻahu	Ellen, 1993
10.9	0.1	-	$1.1–1.3\times10^6$	Valley depth	West Maui	This study
47.9	0.05	0.15	$0.4–1.3\times10^4$	He^3	Hanalei, Kauaʻi	Ferrier and others, 2013
82.0	0.13	-	1×10^4	Ca weathering	Kāneʻohe, Oʻahu	Moberly, 1963
100	0.1	-	1×10^2	Alluvial sediment volume	Lānaʻi	Wentworth, 1925
42.9	0.02	-	3×10^1	Alluvial sediment volume	Oʻahu	McMurtry and others, 1995
10.4	0.1	0.3	1×10^1	^{137}Cs	North Hālawa, Oʻahu	Hill and others, 1997
47.9	0.01	0.02	6×10^0	Landslide volume	Hanalei, Kauaʻi	Ferrier and others, 2013
2.5	0.72	-	6×10^0	Suspended-sediment yield	Haiku Stream nr Heeia	PIWSC data
13.7	0.50	-	6×10^0	Suspended-sediment yield	Kawela Gulch near Moku	PIWSC data
47.9	0.39	-	5×10^0	Suspended-sediment yield	Hanalei River near Hanalei	PIWSC data
10.4	0.29	-	18×10^0	Suspended-sediment yield	N. Halawa Stream near Honolulu	PIWSC data
11.1	0.26	-	10×10^0	Suspended-sediment yield	Kipapa Stream near Wahiawa	PIWSC data
116.9	0.26	-	23×10^0	Suspended-sediment yield	Waikele Stream at Waipahu	PIWSC data
2.9	0.25	-	9×10^0	Suspended-sediment yield	Right Branch Kamooalii Str nr Kaneohe	PIWSC data
1.1	0.17	-	8×10^0	Suspended-sediment yield	Luluku Stream at Altitude 220 ft near Kaneohe	PIWSC data
12.1	0.17	-	8×10^0	Suspended-sediment yield	N. Halawa Stream near Quarantine Station	PIWSC data
9.9	0.12	-	9×10^0	Suspended-sediment yield	Kamooalii Stream below Luluku Stream nr Kaneohe	PIWSC data
2.4	0.05	-	5×10^0	Suspended-sediment yield	Moanalua Stream near Kaneohe	PIWSC data
100	0.04	0.19	$1–2\times10^0$	Sediment and ion yield	Hawaiian Islands	Li, 1988

Acknowledgments

We thank U.S. Army Corps of Engineers and Athline Clark for support for fieldwork from Military Interdepartmental Purchase Request WX3JR941678572. We thank USGS Pacific Coral Reefs project for rain gage and other equipment grants and for salary support for Jonathan Stock. Ron Rickman from the USGS Pacific Islands Water Science Center provided suspended-sediment data for Hawaiian streams. We thank Maui Land and Pineapple Company, Department of Hawaiian Homelands, and Hawaii Department of Land and Natural Resources for enabling land access. Chris Brosius and the rest of the West Maui Mountain Watershed Partnership staff provided facilities, logistical support, and back-country access. An early and exhaustive review by Patrick Muffler (USGS) dramatically improved this manuscript. We thank Oliver Chadwick (University of California, Santa Barbara) and Katherine Skalak and Mark Landers of the USGS for very helpful reviews. Faults in interpretations and errors are those of the first author.

References Cited

Chen, Y.R., and Chu, P.-S., 2014, Trends in precipitation extremes and return levels in the Hawaiian Islands under a changing climate: International Journal of Climatology, v. 34, p. 3913–3925.

Dietrich, W.E., and Dunne, T., 1978, Sediment budget for a small catchment in mountainous terrain: Annals of Geomorphology Supplement, v. 29, p. 191–206.

Ellen, S.D, Mark, R.K., Cannon, S.H., Knifong, D.L., 1993, Map of debris-flow hazard in the Honolulu District of Oahu, Hawaii: U.S. Geological Survey Open-File Report 93–213, 28 p., available at http://pubs.usgs.gov/of/1993/of93-213/.

Ferrier, K.L., Perron, J.T., Mukhopadhyay, S., Rosener, M., Stock, J.D., Huppert, K.L., Slosberg, M., 2013, Covariation of climate and long-term erosion rates across a steep rainfall gradient on the Hawaiian island of Kaua‘i: Geological Society of America Bulletin, v. 125, p. 1146–1163.

Gilbert, G.K., 1909, The convexity of hilltops: Journal of Geology, v. 17, p. 344–350.

Green, R.E., Ahuja, L.R., Chong, S.-K., and Lau, L.S., 1982, Water conduction in Hawaii oxic soils: University of Hawaii at Manoa, Water Resources Research Center Technical Report 143, 122 p.

Hill, B.R., Fuller, C.C., and DeCarlo, E.H., 1997, Hillslope soil erosion estimated from aerosol concentrations, North Halawa Valley, Oahu, Hawaii: Geomorphology, v. 20, p. 67–79.

Li, Y.-H., 1988, Denudation rates of the Hawaiian Islands by rivers and groundwaters: Pacific Science, v. 42, p. 253–266.

McMurtry, G.M., Snidvongs, A., and Glenn, C.R., 1995, Modeling sediment accumulation and soil erosion with 137Cs and 210Pb in the Ala Wai Canal and central Honolulu watershed, Hawai‘i: Pacific Science, v. 49, p. 412–451.

Moberly, R., Jr., 1963, Rate of denudation in Hawaii: Journal of Geology, v. 71, p. 371–375.

National Oceanic and Atmospheric Administration, [2014], Climate Data Online: National Centers for Environmental Information database [formerly National Climatic Data Center], accessed July 25, 2014, at http://www.ncdc.noaa.gov/cdo-web/.

Patterson, S.H., 1971, Investigations of ferruginous bauxite and other mineral resources on Kauai and a reconnaissance of ferruginous bauxite deposits on Maui, Hawaii: U.S. Geological Survey Professional Paper 656, 74 p.

Roering, J.J., Kirchner, J.W., and Dietrich, W.E., 1999, Evidence for nonlinear, diffusive sediment transport on hillslopes and implications for landscape morphology: Water Resources Research, v. 35, p. 853–870.

Sherrod, D.R., Sinton, J.M., Watkins, S.E. and Brunt, K.M., 2007, Geologic Map of the State of Hawai‘i: U.S. Geological Survey Open-File Report 2007–1089, pamphlet 83 p., 8 pls., scales 1:100,000 and 1:250,000, available at http://pubs.usgs.gov/of/2007/1089/.

Stearns, H.T., and Macdonald, G.A., 1942, Geology and ground-water resources of the island of Maui, Hawaii: Hawaii (Terr.) Division of Hydrography Bulletin 7, 344 p., 2 folded maps in pocket, scale 1:62,500.

Stock, J.D., Hanshaw, M.N., Rosener, M., Schmidt, K.M., Brooks, B.A., Tribble, G., and Jacobi, J., 2009, Hillslope-channel coupling in a steep Hawaiian catchment accelerates erosion rates over 100-fold [abs.]: American Geophysical Union, Fall Meeting 2009 Abstracts, abstract no. EP53E-04, available at http://abstractsearch.agu.org/meetings/2009/FM/EP53E-04.html.

Stock, J.D., Rosener, M., Schmidt, K.M., Hanshaw, M.N., Brooks, B.A., Tribble, G., and Jacobi, J. 2010, Sediment budget for a polluted Hawaiian reef using hillslope monitoring and process mapping [abs.]: American Geophysical Union, Fall Meeting 2010 Abstracts, abstract no. EP22A-01, available at http://abstractsearch.agu.org/meetings/2010/FM/EP22A-01.html.

Stock, J.D., and Tribble, G., 2010, Erosion and sediment loads from two Hawaiian watersheds, *in* Joint Federal Interagency Conference, 2nd, Las Vegas, Nev., June 27–July 1, 2010, Proceedings: Advisory Committee on Water Information (accessed April 13, 2015 at http://www.acwi.gov/sos/pubs/2ndJFIC/Contents/11D_Stock_02_28_10.pdf).

van Genuchten, M.Th., 1980, A closed-form equation for predicting the hydraulic conductivity of unsaturated soils: Soil Science Society of America Journal, v. 44, p. 892–898.

Timm, O.E., Takahashi, M., Giambelluca, T.W., and Diaz, H. F., 2013, On the relation between large-scale circulation pattern and heavy rain events over the Hawaiian Islands—Recent trends and future changes: Journal of Geophysical Research—Atmospheres, v. 118, no. 10, p. 4129–4141.

Wentworth, C.K., 1925, The Geology of Lanai, Bishop Museum Bulletin, v. 24, 72 p.

Appendix

Appendix

Table A1. Annual totals of intense rainfalls, Lahaina, West Maui.

[mm, millimeters; mm/hr, millimeters per hour; bold indicates largest events]

Water year	Total rainfall (mm)	Sustained rainfall >20 mm/hr (in hours)	Total hours of rainfall above intensity threshold			
			20 mm/hr	30 mm/hr	40 mm/hr	50 mm/hr
1978	76	0	1.25	0.75	0.75	0.25
1979	373	0	4	1	0.75	0
1980	333	0	4.75	2	0.25	0.25
1981	104	0	1	0.5	0	0
1982	508	**4.5**	7.75	3.25	1.75	0.75
1983	239	1.25	2.75	1.75	0.75	0.25
1984	318	3	5.25	2.5	1.25	0.75
1985	109	0	0.75	0.5	0.25	0.25
1986	292	1	3	1	0.75	0.5
1987	206	0	2.25	0.25	0	0
1988	307	1	3.5	1	0.75	0.5
1989	653	**3.75**	10.75	3	1.25	1
1990	526	3	7.5	3.5	2.5	1.25
1991	447	0	6.25	3.5	2	1.25
1992	155	0	1.75	1.25	1	0.5
1993	221	0	2.75	0.75	0.5	0.25
1994	173	0	2	0.5	0.25	0
1995	112	0	3.5	0.75	0.25	0
1996	254	0	2.75	1	0.5	0.25
1997	630	1.25	7.25	2.5	**1.5**	0.75
1998	43	0	0.5	0	0	0
1999	145	1.25	1.5	0.75	0.5	0.5
2000	51	0	0.5	0	0	0
2001	137	0	3.25	0.5	0.25	0

Table A2. Annual totals of intense rainfalls, Puu Kolii, West Maui.

[mm, millimeters; mm/hr, millimeters per hour]

Water year	Total rainfall (mm)	Sustained rainfall >20 mm/hr (in hours)	Total hours of rainfall above intensity threshold			
			20 mm/hr	30 mm/hr	40 mm/hr	50 mm/hr

Table A3. Annual totals of intense rainfalls, Field 28, West Maui.

[mm, millimeters; mm/hr, millimeters per hour]

Water year	Total rainfall (mm)	Sustained rainfall >20 mm/hr (in hours)	Total hours of rainfall above intensity threshold			
			20 mm/hr	30 mm/hr	40 mm/hr	50 mm/hr
2006	1,107	7.25	0	5	3.75	2.5
2007	1,100	8.25	3.75	3.75	2	1.25
2008	1,580	17	2.5	8.25	4.75	2.75
2009	1,295	7.75	0	3.25	1.75	1.25
2010	658	3.25	1	1	1	1
2011	917	6.5	1.25	3.25	1.5	1
2012	1,011	6.75	2.5	2.25	1.25	1
2013	470	1	0	0	0	0

Table A4. Annual totals of intense rainfalls, Field 46, West Maui.

[mm, millimeters; mm/hr, millimeters per hour]

Water year	Total rainfall (mm)	Sustained rainfall >20 mm/hr (in hours)	Total hours of rainfall above intensity threshold			
			20 mm/hr	30 mm/hr	40 mm/hr	50 mm/hr
1978	1,290	10.25	0	6.25	6.25	5
1979	2,443	21	2.25	12	9.25	7.25
1980	3,449	31	1	13	9.5	7.25
1981	1,191	8.5	0	3.5	2	1.25
1982	3,360	37	3.75	15.5	8.75	6
1983	2,017	17.5	0	8.5	5.25	4
1984	1,905	14.75	1.25	10	7.25	5.5
1985	1,542	7.25	0	2	1	0.75
1986	2,360	17	1	4.25	1.5	0.25
1987	2,060	25	6.5	10.25	6	3
1988	2,530	17.5	3.25	6	3	1.5
1989	2,944	24.25	4.75	7.75	5.25	3.25
1990	1,727	8	1.25	3	1.25	0.5
1991	2,400	19.5	3.25	4.5	1	1
1992	1,372	7.5	0	1.25	0.75	0.25
1993	1,890	14.5	4.5	4.25	2.5	1
1994	1,262	6.75	0	2	0.75	0
1995	1,293	8.25	0	1.25	0.5	0.25
1996	1,562	11.75	1	3.25	1.75	0.75
1997	1,725	15.25	2.5	3.75	1	0.25
1998	1,443	7.25	0	1.25	0.5	0
1999	940	7.5	0	1.25	0.25	0
2000	968	6.5	0	1.25	0.25	0
2001	841	2.25	0	1	0.5	0.25
2002	892	5.5	2.75	3	2.5	1.25
2003	1,384	13.5	9.25	5.5	2.75	1.25
2004	1,585	17.5	7.75	6	4	2
2005	1,750	12	0	2.5	0.75	0.25

Table A5. Record of heaviest rainfalls over 1 hour in Lahaina, West Maui.

[mm, millimeters; mm/hr, millimeters per hour; bold indicates largest events]

Time at end of storm	Water year total rainfall at end of storm (mm)	Durations of rainfall above intensity threshold		
		20 mm/hr	30 mm/hr	40 mm/hr
1/7/1982 6:45	30	1	-	-
1/21/1982 14:00	178	1.75	-	-
1/22/1982 5:00	249	1.75	-	-
12/23/1982 20:30	175	1.25	-	-
12/25/1983 2:45	91	1.75	-	-
12/25/1983 5:15	140	1.25	-	-
10/18/1985 7:30	117	1	-	-
11/14/1987 18:45	56	1	1	-
11/4/1988 14:30	74	1.75	-	-
12/16/1988 9:00	292	1	-	-
2/2/1989 21:15	378	1	-	-
10/9/1989 0:45	142	1.5	-	-
12/9/1989 11:45	292	1.5	1	-
1/20/1997 1:15	**472**	**1.25**	**1.25**	**1.25**
12/31/1998 7:15	74	1.25	-	-

Table A6. Record of heaviest rainfalls over 1 hour in Puu Kolii, West Maui.

[mm, millimeters; mm/hr, millimeters per hour; bold indicates largest events]

Time at end of storm	Water year total rainfall at end of storm (mm)	Durations of rainfall above intensity threshold		
		20 mm/hr	30 mm/hr	40 mm/hr
1/1/2004 14:15	246	1.25	-	-
1/3/2004 0:45	424	1.25	-	-
3/22/2004 5:15	859	1.25	-	-
3/24/2006 3:00	338	1.25	-	-
10/16/2006 5:30	48	1	1	-
11/2/2006 14:00	**226**	**1.75**	**1.5**	-
11/28/2007 12:00	99	1.25	-	-
12/5/2007 11:00	**312**	**2**	**1.75**	-

Table A7. Record of heaviest rainfalls over 1 hour in Field 28, West Maui.

[mm, millimeters; mm/hr, millimeters per hour; bold indicates largest events]

Time at end of storm	Water year total rainfall at end of storm (mm)	Durations of rainfall above intensity threshold		
		20 mm/hr	30 mm/hr	40 mm/h
11/2/2006 14:30	**221**	**1.5**	**1**	**1**
12/2/2006 7:00	389	1.25	-	-
3/10/2007 3:00	709	1	-	-
12/5/2007 11:00	**582**	**2.5**	**2.25**	**2**
12/3/2009 23:15	251	1	-	-
1/13/2011 4:00	630	1.25	-	-
10/31/2011 22:45	74	1	-	-
12/13/2011 11:15	345	1.5	-	-

Table A8. Record of heaviest rainfalls over 1 hour in Field 46, West Maui.

[mm, millimeters; mm/hr, millimeters per hour; bold indicates largest events]

Time at end of storm	Water year total rainfall at end of storm (mm)	Durations of rainfall above intensity threshold		
		20 mm/hr	30 mm/hr	40 mm/h
1/11/1979 17:30	513	1	-	-
2/21/1979 5:45	1,328	1.25	-	-
3/16/1980 17:45	1,714	1	-	-
1/25/1982 5:30	1,135	1	-	-
2/11/1982 6:15	1,420	1.5	1.5	-
8/1/1982 10:15	2,962	1.25	-	-
12/25/1983 6:30	737	1.25	-	-
3/19/1986 22:45	1,052	1	-	-
11/10/1986 7:30	272	2.75	2	-
5/5/1987 18:15	1,344	1.25	1.25	-
5/6/1987 4:15	1,438	1	-	-
5/6/1987 10:45	1,524	1.5	-	-
1/1/1988 8:00	**922**	**2**	**1.25**	**1.25**
4/3/1988 6:15	1,778	1.25	-	-
12/16/1988 9:45	424	1.5	-	-
2/2/1989 21:30	859	1	-	-
4/5/1989 3:15	1,471	2.25	-	-
12/9/1989 11:45	274	1.25	-	-
11/19/1990 2:30	488	1	-	-
12/24/1990 1:45	871	1	-	-
9/19/1991 13:00	2,388	1.25	-	-
12/31/1992 1:45	640	1.25	-	-

Table A8. Record of heaviest rainfalls over 1 hour in Field 46, West Maui.—Continued

Time at end of storm	Water year total rainfall at end of storm (mm)	Durations of rainfall above intensity threshold		
		20 mm/hr	30 mm/hr	40 mm/h
7/22/1993 15:15	**1,537**	**1.75**	**1.25**	**1.25**
7/22/1993 19:45	1,590	1.5	-	-
3/30/1996 23:15	1,016	1	-	-
12/14/1996 4:00	**348**	**1**	**1**	**1**
1/4/1997 10:15	668	1.5	-	-
11/27/2001 7:15	381	1.5	1.25	-
5/13/2002 5:15	**617**	**1.25**	**1**	**1**
10/15/2002 7:00	81	1.5	1.25	-
1/24/2003 22:30	419	1	-	-
1/29/2003 23:15	505	1.5	-	-
1/30/2003 4:30	554	1	-	-
2/14/2003 8:45	732	4.25	-	-
12/25/2003 14:00	175	1.25	1	-
12/25/2003 16:15	226	1.5	1	-
2/27/2004 20:30	419	1	-	-
2/27/2004 23:30	478	1.5	-	-
3/22/2004 19:45	937	2.5	-	-

Menlo Park Publishing Service Center, California
Manuscript approved for publication September 29, 2015
Edited by Regan Austin
Layout by Cory Hurd

USGS

Stock and others—**Reconnaissance Sediment Budget for Selected Watersheds of West Maui, Hawai'i**—Open-File Report 2015–1190

ISSN 2331-1258 (online)
http://dx.doi.org/10.3133/ofr20151190